VOL. 15 No. 2, pp. 37-72 AUGUST 1953

Philips Technical Review

DEALING WITH TECHNICAL PROBLEMS
RELATING TO THE PRODUCTS, PROCESSES AND INVESTIGATIONS OF
THE PHILIPS INDUSTRIES

EDITED BY THE RESEARCH LABORATORY OF N.V. PHILIPS' GLOEILAMPENFABRIEKEN, EINDHOVEN, NETHERLANDS

AN ELECTRONIC HEARING AID

by P. BLOM.

621.395.92:534.773.2

Means of compensating auditory deficiencies have been known for some centuries, but until recently these were large and clumsy appliances. The modern electronic hearing aid is small, light and unobtrusive, and it is much wider in its scope. For an electronic hearing aid to have the widest possible field of application it should be easily adaptable to suit the many different forms of deafness that exist. This point is given special consideration in the following description of Philips hearing aids.

The object of a hearing aid is to compensate, in some measure, the auditory deficiency in persons who are hard of hearing. The hearing aid is thus an amplifier of sounds, designed for one specific purpose. Such appliances have been known for some centuries, and everyone will remember the large trumpets which were still in use not so very long ago; their origin, of course, goes back much further than the seventeenth century ear trumpet shown in *fig. 1*. It is only within the last two decades that acoustic amplification has been achieved by electronic means. The advantages of electronic hearing aids are manifold; they are smaller, lighter and less obtrusive.

In this article a new hearing aid is described (marketed in three models, *fig. 2*), which differs in certain respects from earlier types. Every effort has been made to ensure not only compactness and low current consumption, but also the widest possible range of application. The design of the instrument provides for automatic volume compression based on several control levels, and a wide choice of response curves. A special characteristic of the design is the method of construction and assembly, which allows for the easy replacement of components and gives a high degree of resistance to tropical conditions.

A brief discussion of the human ear and the defects of hearing will first be given as an

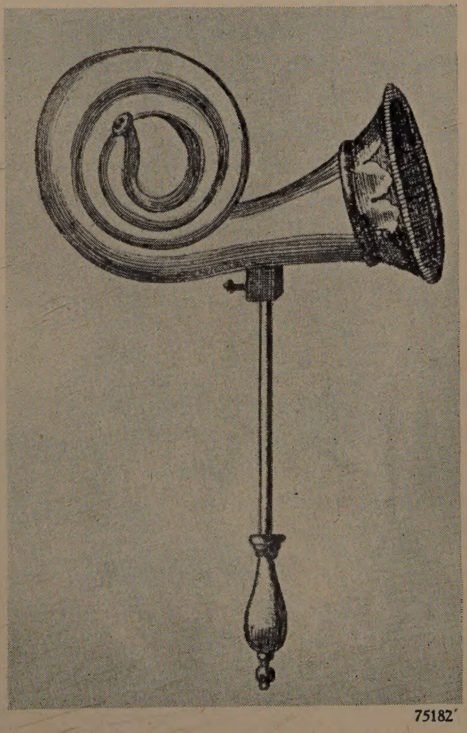

Fig. 1. Design for a hearing aid by A. Kirchner, 1684. (From G. v. Bekesy and W. A. Rosenblith, Early history of hearing: Observations and theories, J. Acoust. Soc. Amer. **20**, 727-748, 1948.)

introduction to the subject. A description follows of the technical features of the hearing aid and the miniature components which were specially designed for this instrument.

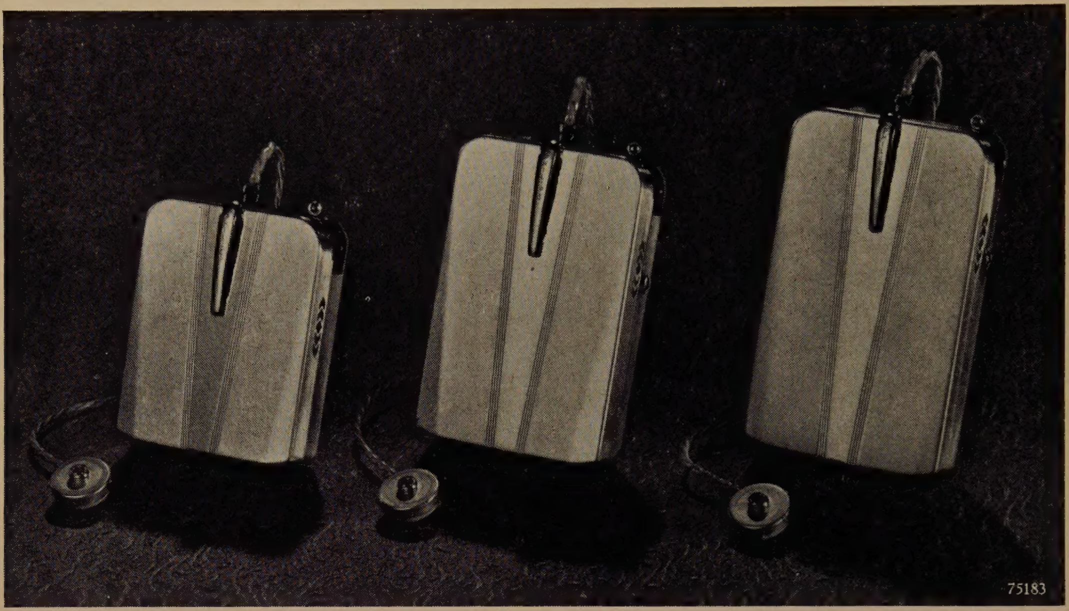

Fig. 2. The three models of new Philips hearing aid. The microphone slots are seen on the right-hand side, and the volume/tone control in the top right-hand corner. The switch next to the microphone slots operates the listening coil.

The organ of hearing

The human ear consists in the main of three parts, each of which can be regarded as quite distinct from the others (*fig. 3*). Starting from the outside we have first the outer ear which comprises the auricle or shell of the ear, and the auditory passage. The air vibrations of which sounds consist are collected by the auricle and are directed through the auditory passage to the middle ear, which is separated from the outer ear by the ear drum. The middle ear comprises the three well-known bones or ossicles of the ear. These ossicles serve to transfer the vibrations of the ear drum, as produced by the sound, to the membrane of the fenestra ovalis, an oval aperture which forms the connection with the inner ear. The inner ear communicates with the cavity of the nose and throat through the Eustachian tube and so prevents differences of pressure from occurring in the vestibule of the inner ear. Within the inner ear there is a spirally coiled duct of about $2^{1}/_{2}$ turns, narrowing towards the upper end, known as the cochlea. Now, the cochlea is divided lengthwise in two parts by a membrane, one half of which communicates with the fenestra ovalis and the other with a second aperture in the wall of the inner ear, the fenestra rotunda. The membrane is not continued right to the end of the cochlea and the two halves are therefore in communication with each other. The cochlea is filled with a viscous fluid, and the membrane, which is also hollow and filled with fluid, contains the so-called Corti's organ, to which the vibrations are transferred from the fenestra ovalis by the fluid. The cross-section of the cochlea with Corti's organ is not the same throughout its length, and it is due to this fact that each part of this organ responds to a different frequency; that part which is nearest to the fenestra ovalis responds to

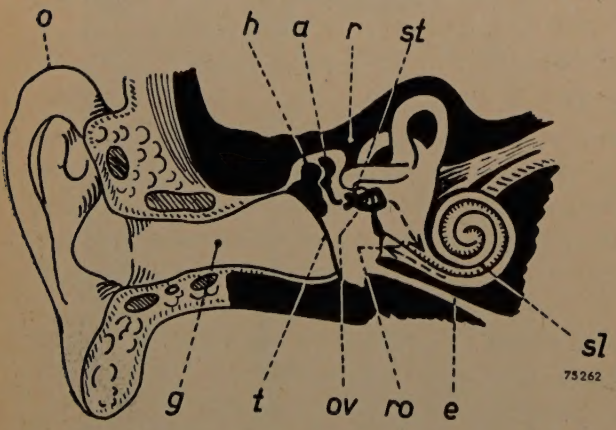

Fig. 3. Diagram of the human ear. *O* auricle; *g* auditory passage; *h* hammer; *a* anvil; *st* stirrup; *t* ear drum; *ov* fenestra ovalis; *ro* fenestra rotunda; *sl* cochlea; *e* Eustachian tube; *r* petrosal bone.

the very high frequencies, whereas the top of the cochlea is sensitive to very low frequencies. This mechanical selection of sounds within the cochlea is quite rough, but it is followed by a much finer, but as yet little understood process of selection by the auditory nerve, with which the cells of Corti's organ are in communication. The auditory nerve passes the sound stimuli to the brain, where the sound "signal", analyzed into its various component frequencies, is received; in this way we are enabled to form conclusions as to the quality and origin of a sound.

So far only air-conducted sounds have been mentioned, but sound can also reach Corti's organ by conduction through the bones of the skull (bone-conduction); by this means, however, it is mainly the lower frequencies that are perceived.

Defects of the ear may result in varying degrees of deafness and can be placed in three categories, viz. deficiencies in the conduction of the sound, causing conduction deafness; defects of the cochlea or auditory nerve, resulting in perception deafness; and defects of the brain. The last-mentioned will not be considered, as this cannot be made good by means of a hearing aid.

Conduction deafness may be caused by wax blocking the auditory passage, or it may occur as a result of inflammation. The ear drum can also be a source of conduction deafness, e.g. when wax is deposited on it. Another frequent cause is inflammation of the middle ear, possibly with rupture of the eardrum. Usually this kind of deafness is only temporary, but it can also be permanent (chronic inflammation).

A stoppage in the Eustachian tube, resulting in pressures below atmospheric in the cavity of the middle ear will also be accompanied by deafness.

Otosclerosis, a disease of the middle ear manifested in a morbid growth of bone, will sometimes hamper the movement of the auditory ossicles; in many cases this can be overcome by an ingenious operation known as fenestration.

In all these instances it is mainly the air conduction that is impeded or ceases to function altogether.

Perception deafness is frequently caused by a gradual degeneration of Corti's organ; usually this commences at the point where the higher frequencies are registered, and gradually progresses into the region of the lower frequencies. Curiously enough, however, at high sound *intensities*, high tones can still often be heard, and at their full strength too. There is then an abrupt transition between deafness and hearing (*fig. 4*). Since the threshold of pain (the maximum sound intensity which may reach the ear without causing actual pain) usually remains at the same level, the range or span of sound intensities that the sufferer can perceive is greatly reduced. This effect is known as regression.

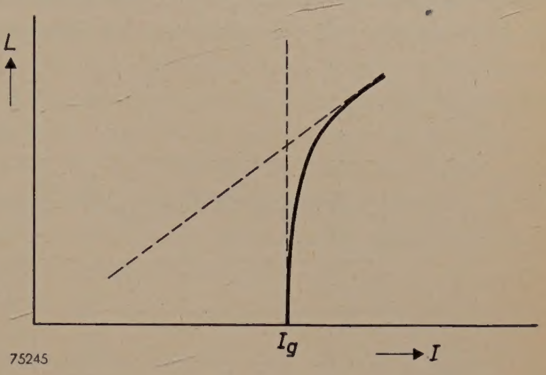

Fig. 4. The effect of regression. Loudness L as heard by the patient plotted against the sound intensity I in the auditory passage. Below a certain intensity I_g the patient hears little or no sound; above that point the hearing is comparable with that of a person with normal hearing.

In order to diagnose the nature of a deficiency in hearing, a chart is plotted for the auditory loss of the sufferer, for both air-conduction and bone-conduction, as a function of the frequency of the submitted sound. The auditory deficiency is defined as the ratio of intensities that can just be perceived by the patient, to those in the case of a person of normal hearing; this is expressed in decibels. The curve thus obtained is known as an audiogram and it is plotted with the aid of an instrument called an audiometer [1]). A number of audiograms are depicted in *fig. 5*, and from these it is seen that in serious cases of conduction deafness the sound pressure required to produce a sensation that is only just perceptible can be up to 60 dB, i.e. roughly 1000 times stronger than for persons with normal hearing. A pronounced dependence on frequency is not usually apparent. Perception deafness is distinguished from conduction deafness by the fact that hearing is impaired in both air-conduction and bone-conduction; this can be seen from the audiograms — as a rule, in conduction deafness, bone-conduction suffers no attenuation (2, fig. 5). As already mentioned, perception deafness is usually more evident in the higher frequencies, and in that region it may be absolute, i.e. more than 100 dB.

Many cases of deafness are of a mixed type, as will be seen from fig. 5. Regression cannot be diagnosed from a single audiogram; more extensive tests are essential when an examination is to be made.

---

[1]) An instrument of this type is described in an earlier number of this Review; see L. Blok and H. J. Köster, Philips tech. Rev. **6**, 234-239, 1941.

The task of the hearing aid

The main function of a hearing aid is to so amplify sounds that speech will be intelligible and that local noises will give the user an impression of what is going on around him. The reproduction of music takes second place.

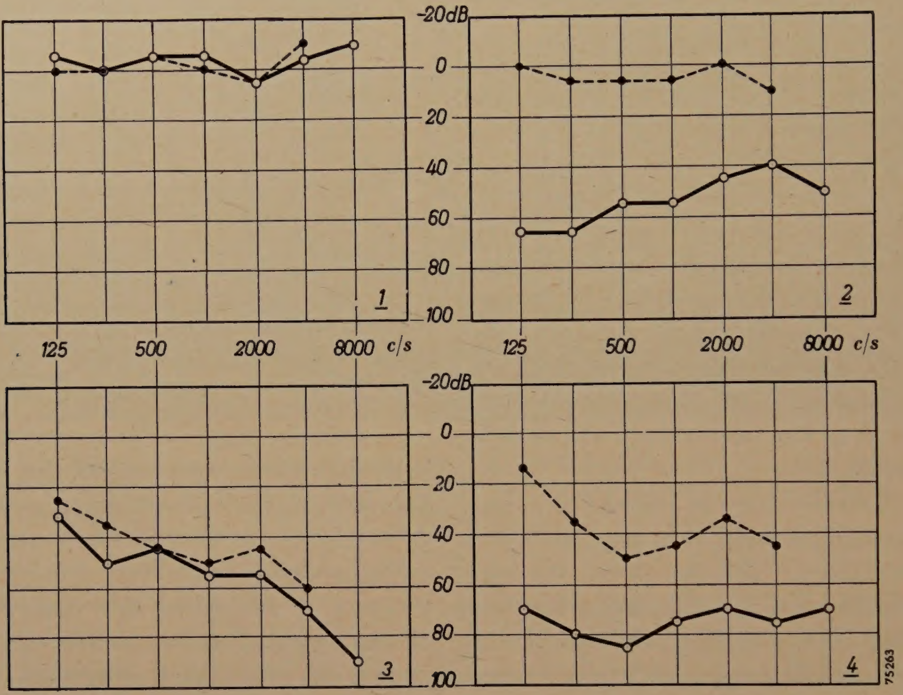

Fig. 5. Audiograms. Auditory deficiency in dB (vertical) compared with the average sensitivity of the human ear, as a function of the frequency of the sound in c/s (horizontal). Chart *1* represents normal hearing; *2* a person with conduction deafness; *3* a person with perception deafness and *4* a sufferer from a mixed form of deafness. The full lines refer to air-conducted sound and the bröken lines to bone conduction. This figure consistsex of amples only: each particular form of deafness yields its own audiograms.

From the foregoing brief review of the major forms of deafness it will be clear that the individual requirements to be imposed on a hearing aid must differ very considerably between one case and another. In addition, it has not yet been found possible to establish any well-defined relationship between the nature of a deficiency in hearing as characterized by the audiogram, and the optimum characteristics required of the hearing aid by the user. For example, chart *3* in fig. 5 would indicate the need, on physical grounds, for a hearing aid with a rising amplification factor (rising frequency response curve), but very often, if not invariably, the patient will give preference to a flatter characteristic.

One of the difficulties in determining the most desirable characteristic for a hearing aid is the fact that the hearing of a deaf person using a hearing aid is monaural. In monaural hearing several curious effects become apparent. The usual directional effect largely disappears, although with some practice this can be recovered. Turning of the microphone produces differences in the quality of the signal as received, since the response curve of the instrument depends to a certain extent on the direction from which the sound is picked up 2)). Another effect of monaural hearing is the apparent reception of all local sounds from one and the same plane; in other words, the user of the hearing aid is not well able to determine the distance from the sound source, although here, too, a certain amount of judgment is restored in most cases, after some practice.

---

2) See also K. de Boer and A. Th. van Urk, Some particulars of directional hearing, Philips tech. Rev. 6, 359-364, 1941.

As it is only the patient himself who can be the ultimate judge of the most desirable characteristics for the hearing aid, it is most essential that the characteristic should be variable within wide limits. This applies not only to the response curve, but also to other characteristics. Manufacturers would be able to meet the need for variable characteristics very easily were it not for the fact that they are tied in two respects. First, from the point of view of the user, certain other requirements have to be met, which are also quite important, e.g. lowest possible current consumption, small dimensions, lightness, robustness etc. In view of this it is usual to limit amplification to a range of frequencies of from 100 to 5000 c/s, but even then it is very difficult to adequately fulfil all the requirements mentioned.

Secondly, it is important to the manufacturers themselves to be able to meet the needs of the greatest possible number of users with only one type of hearing aid. In other words, their aim is to cover the various needs with a single type of instrument, capable of simple manual adjustment. This facilitates mass production and reduces costs.

Some details now follow of the manner in which these several requirements have been met in the Philips hearing aid.

Scope of the hearing aid

The basic requirement for the response of a hearing aid may be said to be an amplification of 50 dB in a frequency range of 200-4000 c/s (which includes speech and local sounds). Care must be taken, however, that the sound of loud shouting (input sound intensity about 30 dB above normal speech intensity), or of other very loud sounds, is not distorted, and that the user does not receive such a volume of sound that the threshold of pain is passed. The need for such control on the volume is particularly evident among sufferers from regression deafness, for their margin between the thresholds of hearing and pain is usually smaller than the range of intensities of the sounds which are to be rendered audible.

Control on the amplification can be either abrupt or continuous; the former method is known as signal cut-off, which implies that the signal is prevented from exceeding a certain value at the output. *Fig. 6* illustrates a signal subjected to cut-off; it will be seen that considerable distortion is introduced, and this affects the clarity of reproduction. In the Philips instrument, therefore, the continuous method has been adopted, viz. automatic volume compression, as this avoids distortion. In addition, the operating level of the control is variable in seven stages, to meet the need for versatility explained above.

Modification of the response curve of the Philips hearing aid can be effected in the first place by means of a tone switch. The user is thus given the facility of selection from three response characteristics to suit his particular need, the difference between the characteristics lying mainly in the limits of the frequency range. Of even greater importance is the fact that when purchasing his hearing aid the user is given a choice of seven earphones, each having an entirely different response curve. In all, therefore, a selection can be made from 3 × 7 = 21 overall characteristics.

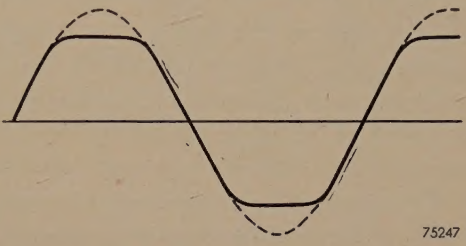

Fig. 6. Illustrating the distortion arising from abrupt cut-off of the output signal.

The microphone, pick-up coil and earphone

The microphone in the Philips hearing aid is of the crystal type, all the components being so assembled as to form a complete removable unit. A diagram of the microphone is given in *fig*. 7. The "capsule" of the microphone consists of a round housing in which the acoustically sensitive element, a square crystal of Rochelle salt (sodium potassium tartrate) is mounted. The capsule is mounted flexibly in a rectangular housing which also carries contact pins for connections to the amplifier. Sound vibrations are picked up by a small conical diaphragm of aluminium foil which is connected to one corner of the crystal. The electrical connections through the round and rectangular housings are insulated

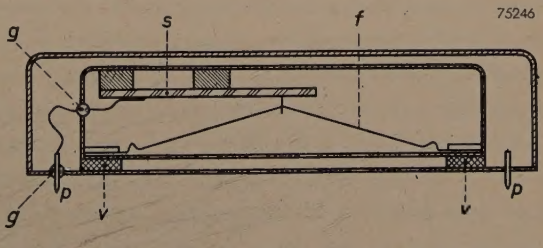

Fig. 7. Cross section of the microphone in Philips hearing aid. *s* Rochelle salt crystal; *f* aluminium foil; *v* resilient suspension of housing with crystal and foil; *g* glass beads; *p* contact pins.

with glass "bead" bushings which also serve to seal the casing against moisture.

A large part of the background noise that users of hearing aids always hear is produced by friction between the clothing and the microphone or neighbouring parts of the instrument ("case noise"). In order to suppress such noise as much as possible in the new hearing aid, the slots for the microphone are situated in the side of the case.

Rotation of a switch enables the user to connect the microphone to a so-called "pick-up coil". By means of this coil signals may be picked up inductively from the field of an exterior coil, such as that of a telephone receiver. The pick-up coil has a large number of turns, so that the stray field from a telephone receiver induces a signal voltage which is sufficiently large for the hearing-aid amplifier. In this way the acoustical link between the telephone and the hearing aid, which is responsible for considerable distortion, is eliminated. In addition, the magnetic transfer of the signal effectively eliminates all airborne sound, so that background noise [3]) — unusually distracting in a telephone conversation due to monaural hearing — is greatly reduced.

The pick-up coil is also being used to an increasing extent at concerts and in theatres and churches. A large loop of wire is laid round the walls of the building and connected to the output of an audio-frequency amplifier; the A.F. magnetic field of the loop induces voltages in the pick-up coil. Those who are hard of hearing need thus no longer be restricted to the front row or other specific places, but are free to move about while listening to reproduced sound which is almost wholly free from auditorium noises and reverberation. This system can also be used to great advantage by persons with normal hearing, for example in conducted parties in museums ("radiophonic" address) (*fig. 8*), for communication with personnel in large factory bays where the noise level is high or, again, in television or film studios.

The earphone of the hearing aid is attached to the auditory passage by means of a plastic ear-piece (*fig.9*). The closure should be as nearly as possible airtight in order to avoid loss of sound and distortion.

As already pointed out, the purchaser of the hearing aid has a choice of seven different earphones. Five of these are of the magnetic type with an impedance of 100 Ω (at 1000 c/s) and different response curves; the other two are crystal earphones of 100 000 Ω impedance, giving more output in the higher tones. The crystal receiver is also lighter and smaller than the magnetic one. All these receivers are fitted with a standard press-stud, by means of which the earpiece is attached.

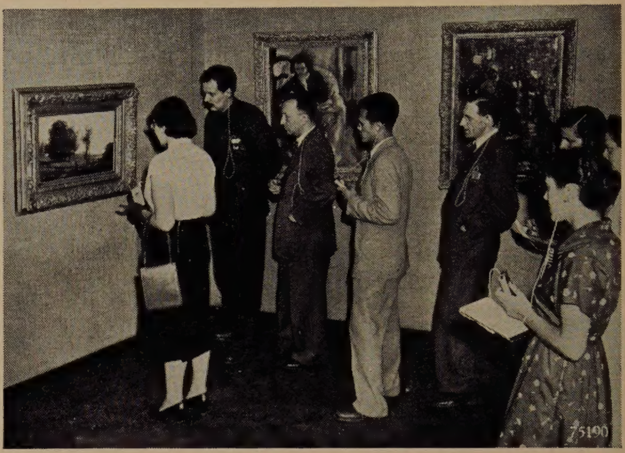

Fig. 8. Visitors to the Municipal Art Gallery, Amsterdam, listening to the "guide" with the Philips hearing aid and pick-up coil.

The amplifier

The amplifier in the Philips hearing aid is of the conventional 3-stage audio-frequency type. The maximum electrical gain is 72 dB, or an amplification of about 4000, which can be reduced manually by means of a volume control situated after the first valve. The average amplitude of the alternating grid voltage as delivered by the microphone is 1 mV for a normal sound level (speech); the A.C. voltage supplied by the output transformer is then about 5 V. Measurement of the sound pressure of the receiver placed in an artificial ear [4]) shows that

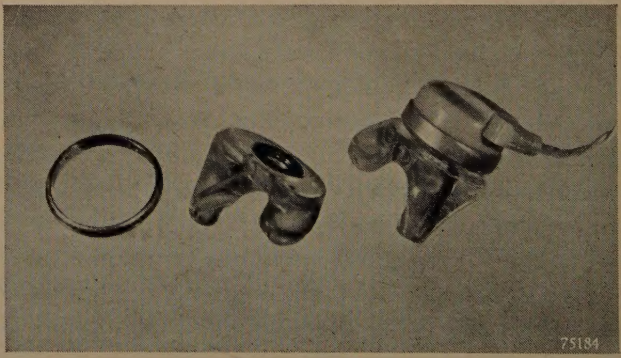

Fig. 9. Plastic ear-piece with press-stud by means of which the receiver is attached to the ear; on the right it is shown with the earphone attached. A wedding ring is shown for comparison.

---

[3]) Local noises can also be excluded by using a throat microphone, see Philips tech. Rev. 5, 6-14, 1940.

[4]) For a description of the artificial ear see K. de Boer and R. Vermeulen, On the improvement of defective hearing, Philips tech. Rev. 4, 316-319, 1939.

the acoustic amplification of the complete hearing aid is 52 dB at 1000 c/s.

The secondary side of the output transformer has an impedance of 100 Ω, matching the impedance of the magnetic earphone. By reversing a plug in its socket the user can increase the impedance at the output terminals of the amplifier to 100 000 Ω, thus providing a matching for a crystal earphone. *Fig. 10* shows the circuit diagram of the complete amplifier.

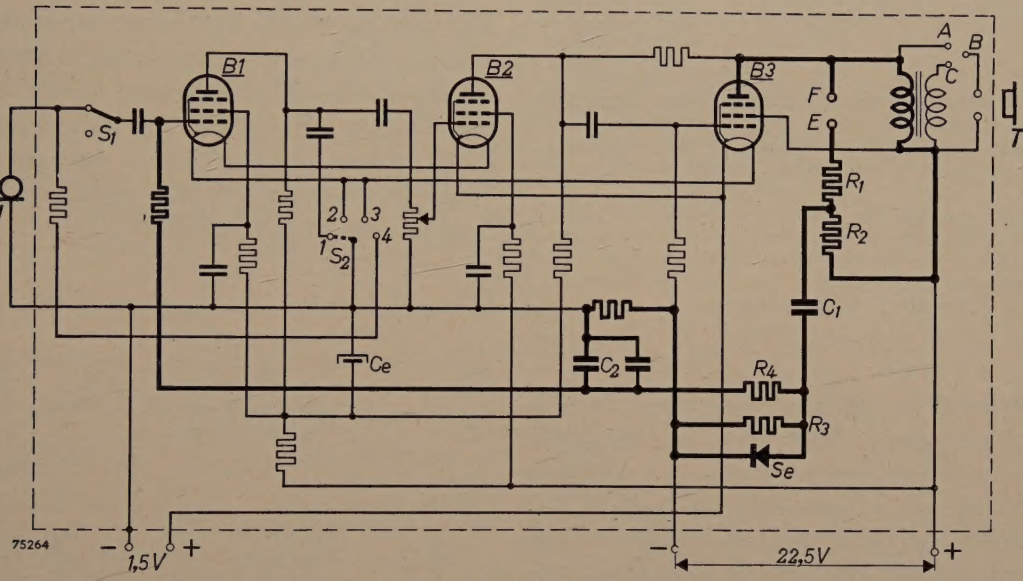

Fig. 10. Circuit diagram of the amplifier. Only the principal components are listed: M microphone; S_1 switch, microphone/pick-up coil (the leads to the pick-up coil are not shown). B_1, B_2, B_3 valves; S_2 tone switch: in position 1 the hearing aid is inoperative. C_e electrolytic decoupling capacitor. A, B, C, E and F contact sockets, strapped by means of a plug. T earphone receiver. The automatic volume compression circuit is indicated by the heavy lines. The alternating anode voltage from the output valve B_3 is fed through R_1 and C_1 to a selenium rectifier Se, and the rectified voltage is applied across R_4 to the grid of the input valve B_1. C_2 and R_4 determine the "attack" time of the compression, and C_2, R_4 and R_3 the "release" time. The control level is determined by the value of resistor R_2.

The automatic volume compression mentioned earlier is provided by that part of the circuit shown by heavy lines in the figure. The alternating anode voltage from the output valve B_3 is taken through R_1 and C_1 to a selenium rectifier Se, which rectifies it, and the resultant D.C. voltage is applied to the grid of the first valve B_1. In this way the bias of the input valve is automatically reduced and the amplification limited when the input voltage rises too much.

It is of course essential that strong sound pulses should be attenuated very quickly, as otherwise the initial components of a word might be distorted (the amplifier would be overloaded). The "attack time" of the A.V.C. is governed mainly by the product of the values of R_4 and C_2, which function as a filter for the control voltage from the selenium rectifier to the input valve. On the other hand, this time should not be too short, as this tends to make the amplifier unstable (motor-boating). This can be avoided, however, by coupling elements of suitable values. In practice an attack time of 150 msec has been found satisfactory.

When the sound reaching the microphone is no longer abnormally loud, the amplification should return to its original level, and the time in which this takes place is the "release time"; in order to avoid a noisy background as a result of the A.V.C. becoming inoperative during the pauses in a sentence, this time must not be too short; it is determined by the time constant of the system C_2, R_4, R_3 in fig. 10, and lies somewhere between $^1/_2$ and 1 second.

Fig. 11 shows the action of the A.V.C. with acoustic pulses applied to the hearing aid. With the control at maximum, the amplifier is overloaded for a very short time and therefore gives a distorted signal only for a few milliseconds.

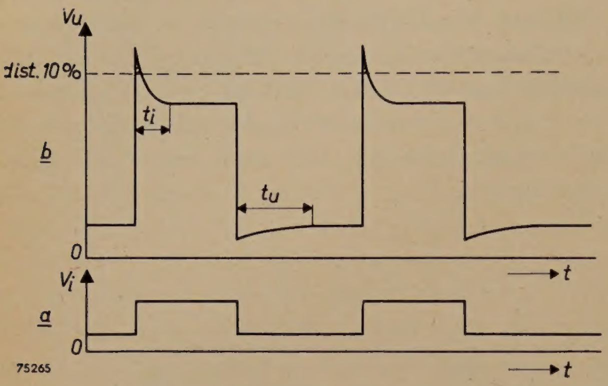

Fig. 11. The action of the automatic volume compression. *a*) A voltage of square wave-form (V_i) is applied to the input of the amplifier, the amplitude being such that, without the A.V.C., the distortion of the output voltage would be more than 10%.
b) The output voltage V_u, with A.V.C. operating, exhibits distortion of more than 10% for only a very short period. The significance of the attack and release times of the A.V.C. (t_i and t_u respectively) is clearly seen from the figure. The scale of t_i is exaggerated in the diagram.

As mentioned above, the control level can be adapted to the needs of the user. This individual matching is accomplished by means of a resistance (R_2, fig. 10) placed in series with the receiver. It is not necessary, nor is it desirable, that the user should have control over all the variables in the instrument: he will obviously never require to adjust the instrument to respond to forms of deafness other than his own. For this reason the output level is pre-set at the time of purchase, while the A.V.C. resistor is provided in the reversible plug to which reference has already been made. The patient, assisted by the doctor, has a choice of 2 × 8 different plugs, which will give him either uncontrolled output, or control in one of seven different ranges, each differing by 5 dB, either with the crystal or the magnetic earphone.

Some response curves for the complete hearing aid are reproduced in *fig. 12;* these show the ratio of output sound pressure to input sound pressure in dB, as a function of the frequency. The characteristics depicted are examples of what can be achieved with the seven-times-three combinations of receiver and tone control. This choice of characteristics, together with the eight ranges of A.V.C., provide a very wide range of application of the instrument, capable of meeting different forms of deafness.

Construction

The construction of the Philips hearing aid differs in some respects from conventional types. Apart from the necessity for small dimensions, robustness, resistance to tropical conditions etc., easy replacement of the components was made an essential feature of the design. If components can be easily replaced, repair work is greatly simplified. The dealer is then in a position to remedy the more usual faults himself with the aid of a manual only, no soldering or measuring instruments being necessary.

The advantages of the interchangeability of the receiver as well as the reversible plug are obvious. The amplifier is composed of units linked mechanically and electrically by contact pins; the batteries form another unit in themselves. Contact pins and springs complete the circuits of the microphone, tone switch etc., which are also separate units. This method of construction has proved a very satisfactory answer to the problem of the simple replacement of components.

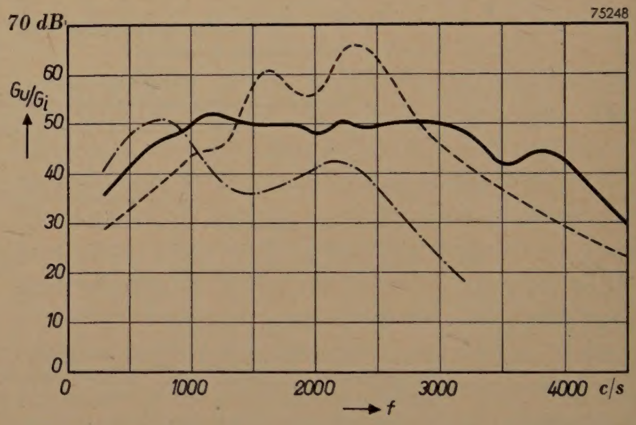

Fig. 12. Response curve of the complete hearing aid for three of the 21 combinations of earphone and tone control setting. The vertical axis represents the acoustic amplification, i.e. the ratio of output sound pressure G_u to input sound pressure G_i, expressed in dB.

Fig. 13 is an exploded view of the various components and shows how they are grouped into their various units. A photograph of the interior of the hearing aid is reproduced in *fig. 14,* which shows the intermediate model of the range of three (see fig. 2 and below). No individual resistors etc. will be seen, either in the exploded diagram or in the photograph, this being due to the special method employed in incorporating them all in their particular unit. The resistors and capacitors, as well as the output transformer, are first laid out on a resin-bonded paper plate (*fig. 15*), all the connections being made on the back of the plate. There is an almost complete absence of soldered joints in this hearing aid: nearly all the leads are spot welded in order to avoid a dangerous rise in temperature during assembly of the components, which are mounted in close proximity to each other. The entire unit is moulded into a block of polyester resin [5]) which is then polymerized; the block thus formed is denoted by *7* in fig. 13. Polyester resins have very excellent insulating, damp-resisting and mechanical properties, closely resembling those of polystyrene and, owing to their low surface tension before polymerization, permeate easily into the small spaces between the components.

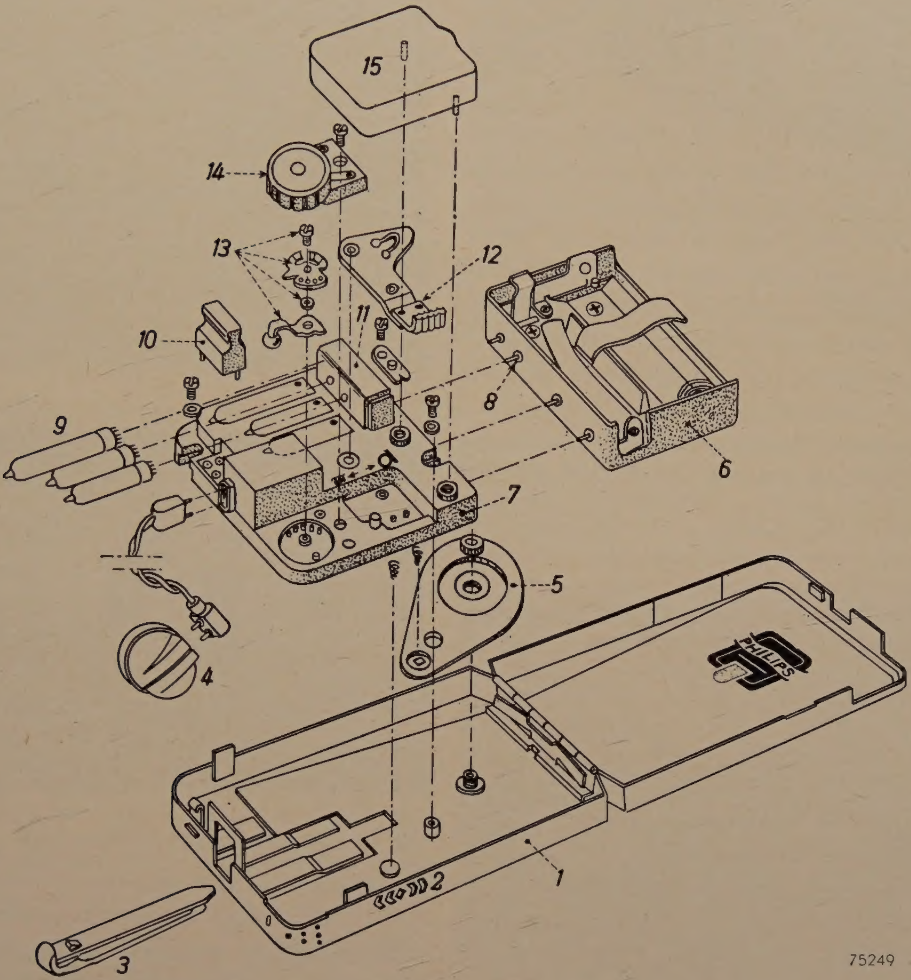

Fig. 13. Exploded view of the Philips hearing aid. The principal components are numbered: *1* case with microphone slots *2*, and clip *3* for attachment to the clothing; *4* earphone with cord; *5* pick-up coil; *6* battery case; *7* block of polyester resin containing the electrical components; *8* contact pins linking the components of the hearing aid electrically and mechanically; *9* valves; *10* plug: *11* valveholder; *12* switch for microphone/pick-up coil; *13* tone switch; *14* volume control. *15* microphone in screened housing.

The local "climate" in which hearing aids are generally used differs considerably from that in which most electronic equipment operates. The set is carried either in the breast pocket, or almost in direct contact with the body. In the latter case a relative humidity of 100% is fairly closely approximated. The temperature differs greatly according to the method of carrying and, when the case is worn close to the body, the possible effects of skin secretions must also be taken into account. All these factors are accentuated in tropical climates. In the design, therefore, allowance has been made for temperature variations between 0 and 45 °C and relative humidities between 0 and 100%. Thermal stability has been ensured by specially designing each component; this will be referred to again later. Sensitivity to humidity is avoided by moulding the moisture-sensitive components into the polyester resin block; judicious selection of the constituents of the resin has yielded a polymerization temperature of only 35 °C, so that damage to the components is avoided and only negligible

---

[5]) See J. P. Mudde, Polyester casting resins, Plastica **6**, 12-15, 1953 (No. 1).

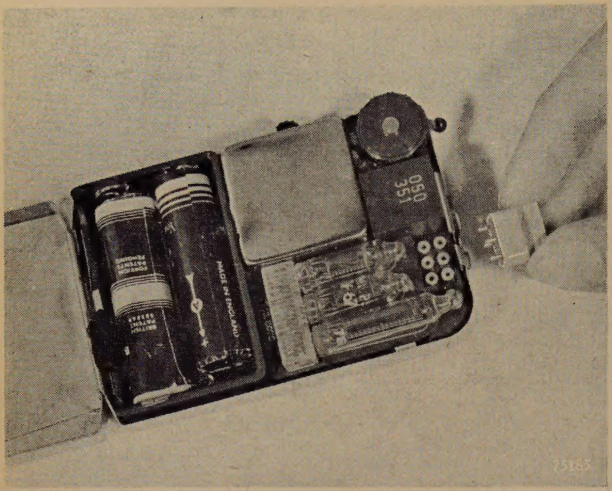

Fig. 14. Interior of Philips hearing aid. Only the screened microphone, the volume control, the valves and their holder, the plug and the batteries can be seen.

shrinkage stresses (on cooling) occur. In order to reduce still further the shrinkage and increase the physical strength, a quantity of ceramic powder ("Kersima" [6]) is added to the moulding powder. This ensures at the same time that the instrument shall be shockproof. Hearing aids belong to a class of equipment which, in contrast to radio receivers for example, are subjected to constant jolting and vibration; robustness, therefore, is an essential requirement.

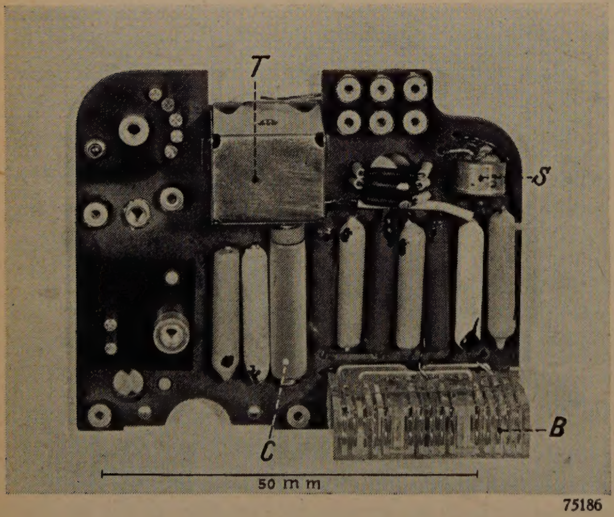

Fig. 15. Assembly of the electrical components on resin-bonded paper plate. The whole is later moulded solid in polyester resin. *T* screened output transformer. *C* electrolytic capacitor; *B* valveholder; *S* selenium rectifier.

The miniature components

The smallness of the hearing aid is due to the very compact design of the components. As standard components would require too much space, an entirely new range of components was designed for the new Philips hearing aid, very small in size, but with excellent electrical properties. The use of these components are not confined to hearing aids alone, for there are many other fields in electronics in which an important outlet for such components exists. The more important components of the hearing aid will now be discussed.

The valves (*fig. 16*) are of course battery valves, of the sub-miniature type. The DF 67 is used in the first and second stages; the output valve is the DL 67, except in the smallest model of the hearing aid which is fitted with the DL 66. The valves are mounted in a special valveholder.

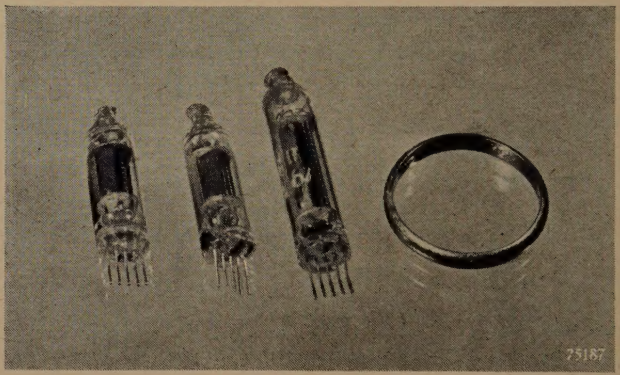

Fig. 16. The three amplifier valves, with a wedding ring for comparison of size. The valve at the right is the output valve DL 67.

The coupling resistors between the three stages of amplification are very small indeed, viz. $7 \times 1^{1}/_{2}$ mm, and are capable of carrying a load of 1/50 W (*fig. 17*). They consist of ceramic tubes coated with graphite suspension, the characteristics of which can be varied to yield resistance values of from 1000 Ω to 15 mΩ. The coupling capacitors, of which a specimen is also shown in fig. 17, are also manufactured from ceramic tube, in this case a grade of "Kersima" of which the dielectric constant is very high, namely 4000. With this material very small capacitors can be made in a range of values up to 6400 pF. The dimensions are $16 \times 3^{1}/_{2}$ mm. A special feature of these components is that the leads are attached inside the tube of the capacitor, leaving the exterior quite smooth. The capacitors are protected by a coating of insulating material and can therefore be mounted in close contact with each other.

---

[6] For a description of different kinds of "Kersima", see R. A. Ijdens, Ceramics and their manufacture, Philips tech. Rev. **10**, 205-213, 1949; E. J. W. Verwey and R. D. Bügel, Ceramic materials with a high dielectric constant, Philips tech. Rev. **10**, 231-238, 1949.

An electrolytic capacitor (*Ce* in fig. 10) is connected in parallel with the anode battery to prevent the amplifier from oscillating (it decouples the anode circuit). There is always some risk of oscillation as the batteries get older; the internal resistance then rises and the coupling between the circuits becomes tighter. Hence the capacitor in the circuit enables the user of the hearing aid to obtain the longest possible service from his batteries, although there is of course a limit, imposed by the ultimate decrease in the amount of power available. The electrolytic capacitor is also quite small; it is housed in an aluminium tube 18 × 4 mm (fig. 17) and is made in two ratings, viz. 2 μF at 25 V and 10 μF at 2 V.

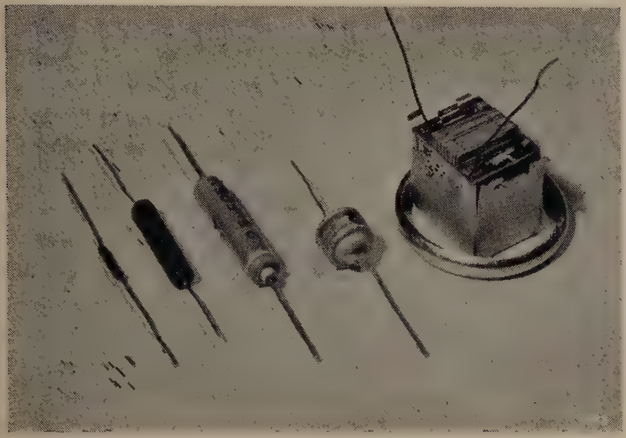

Fig. 17. Miniature components: left to right, carbon resistor, ceramic capacitor, electrolytic capacitor, selenium rectifier and A. F. transformer with part of the screening box removed.

The output valve of the amplifier is matched to the receiver by means of a special transformer (also shown in fig. 17) which provides the impedance matching of 100,000 or 100 Ω. When a crystal receiver is used, the coupling consists only of the self-inductance of the primary winding. Owing to the high impedance of the valve, it is necessary, for effective matching, to provide a high self-inductance; to realize this within small dimensions is made more difficult by the presence of a D.C. component of 200 μA which reduces the permeability of the core. The use of high alloy-content laminations and a large number of turns of very thin wire (30 micron) offers a satisfactory solution. At 1000 c/s the efficiency is 60%, which is high for such a small transformer, being of the same order as that of output transformers of standard dimensions.

As already mentioned, the transformer is moulded into the polyester resin block with the other components; the penetration of the resin guarantees the resistance of this component to tropical conditions.

The amplification of the hearing aid is controlled manually by means of a potentiometer (*fig. 18*) connected between the input and second valves. This is a rotary potentiometer and the physical requirements to be met by this component are fairly heavy. The user is continually adjusting it to give the required volume of sound, and a life of 20,000 operations on both directions is essential. To withstand this a robust spindle bearing is necessary, and fine tolerances on the other parts of the potentiometer. An improved carbon track with a moving carbon contact has practically eliminated potentiometer noise, even for resistances up to 5 MΩ. The amplification between the potentiometer and the output valve is some 400 × , so that it was further necessary to eliminate ripple voltages induced in the grid circuit of the second valve by the output valve. Such voltages could reach the potentiometer through body capacitance via the finger operating the control, and for this reason the potentiometer is provided with an internal screen.

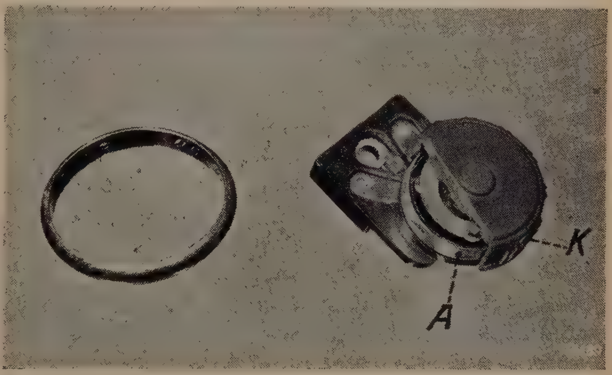

Fig. 18. Volume control with internal screening. The rotary cap *K* is shown cut away to reveal the screening *A*.

The need for such screening could have been avoided by placing the potentiometer between the second stage and the output valve, but strong input signals might then have overloaded the second valve.

To a large extent the dimensions of the hearing aid are dependent on the size of the batteries, two of which are required, viz. one of $1^{1}/_{2}$ V for the filaments and another, of 22 V, for the anodes. As sub-miniature valves are used, very little power is needed (40 mW from the filament battery and 5 mW from the other), so that for a reasonable life, only very small batteries are required (filament battery life about 20 hours; anode battery about 250 hours).

In order to leave the compromise between dimensions and battery life (also economy) to the user, the three models as illustrated were placed on the market, the only difference being in the size of the battery holder (the smallest model, moreover, has no listening coil and is fitted with an output valve of smaller rating). There is accordingly a choice of very small batteries with a correspondingly small case, and larger batteries with larger case, but lower running costs.

Summary. Defects in hearing can assume many different forms. The greater the adaptability of an electronic hearing aid in its applications, therefore, the larger the number of persons who can benefit from it.

This need for adaptability is emphasised in practice by the fact that it has been found impossible to define a unique relation between the desired characteristics of the hearing aid and the nature of the deafness in each individual case. In the new series of hearing aids adaptability is ensured by providing automatic volume compression in a range of seven different levels, from which a selection can be made by ordering the appropriate plug. Further, there is a choice of seven different earphones, five of which are magnetic, and two of the crystal type. These features, in conjunction with a 3-position tone switch offer a total range of 21 different characteristics. The microphone can be switched over to a pick-up coil whereby signals are received directly by induction, for example, from a telephone. In the design of these hearing aids every endeavour has been made to ensure that all the components shall be easily replaceable, so that repairs can be carried out quite simply without any soldering operations. The electrical components are of the miniature type, specially designed for the purpose. All the resistors and capacitors, as well as the output transformer, are moulded into a solid block of polyester resin, ensuring a high degree of robustness and resistance to tropical conditions, and low sensitivity to humidity. All the components, too, were designed with a view to long life and reliable service. Three models of the hearing aid are manufactured, the principal difference between them being in the rating of the batteries.

THREE METHODS OF MEASURING MAGNETIC FIELDS

I. MEASUREMENT BASED ON THE GENERATOR PRINCIPLE

by B. F. JÜRGENS.

II. MEASUREMENT OF THE FIELD ON THE AXIS OF MAGNETIC ELECTRON LENSES

by A. C. van DORSTEN and A. J. J. FRANKEN.

III. MEASUREMENT BY THE PROTON RESONANCE METHOD

by H. G. BELJERS.

621.317.42:538.082

The best method of measuring magnetic field strength depends on the characteristics of the field. Three methods currently employed in the Philips laboratories are described in this article, each of which has its own particular applications. The first method described is suitable for most magnetic circuits and is accurate to within two or three percent. The second was developed specially for measurements on magnetic electron lenses, while the third provides a very accurate absolute measurement of fairly strong homogeneous fields.

Introduction

A large number of methods have been devised for the measurement of magnetic fields and much is still being written on the subject *). When the necessity for such measurements arises in experimental work, special apparatus is often constructed to suit the particular conditions; the need for such special equipment may be due to the fact that the field is restricted within a very confined space, or that measurement is to be effected close to the walls. Examples of such conditions occur in the fields within the air-gaps of electrical machines or moving-coil instruments. The accessibility of the points of measurement will also affect the design of the equipment. For example, the air-gap in an iron circuit will usually be accessible only in a direction at right angles to the lines of force; on the other hand the aperture of a magnetic electron lens is accessible only in a direction parallel to the lines of force. The measurement of inhomogeneous fields also has its own particular problems; here, a certain average value of the magnetic induction over the space occupied by the measuring head is recorded, and there is some uncertainty as to the exact point where the measured value actually exists. Often this difficulty is partly overcome by employing a very small measuring head and, in the first of the methods described in this article, this is the solution adopted. At the same time, it is sometimes possible to determine local values of the field with precision by means of an instrument that is not small, by utilizing certain properties peculiar to the magnetic field. The second method described is an example of this **).

The discovery and study of new phenomena and their behaviour in magnetic fields have again and again led to the development of new kinds of measuring equipment, and this applies to the third method dealt with in this article. This is an incidental outcome of research into the magnetic moments of atomic nuclei. A distinguishing feature of the method is the unusually high degree of accuracy which it offers (within 0.01%).

---

*) A review of practical methods is given by L. W. McKeehan, The measurement of magnetic quantities, J. Opt. Soc. Amer. and Rev. sci. Instr. **19**, 213-242, 1929.

) Another example will be found in W. F. Brown and J. H. Sweer, The fluxball. A test coil for point measurements of inhomogeneous magnetic fields, Rev. sci. Instr. **16, 276-279, 1945.

I. MEASUREMENT BASED ON THE GENERATOR PRINCIPLE

Use is often made of the generator principle to measure magnetic induction [1]). A coil is rotated within the field, about an axis perpendicular to the axis of the coil; the alternating voltage thus generated is proportional to the speed of rotation and also to that component of the induction which is at right angles to the axis of rotation. If the speed be kept constant, the induced alternating voltage is a measure of this component. As a rule a synchro-

---

[1]) A. Kohaut, Ein Messgerät für magnetische Felder, Z. tech. Phys. **18**, 198-199, 1937. R. H. Cole, A magnetic field meter, Rev. sci. Instr. **9**, 215-217, 1938.
O. Klemperer and H. Miller, Search-coil oscillator for measuring fields of magnetic electron lenses, J. sci. Instr. **16**, 121-123, 1939.

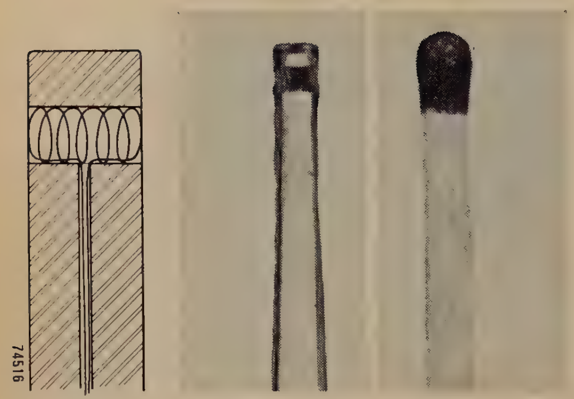

Fig. 1. For measurement of a magnetic field by the generator principle a coil is rotated at constant speed in the field. The coil is mounted in the extremity of a "Perspex" spindle fitted as extension piece to the shaft of a synchronous motor. On the left is an enlarged sketch and in the centre a photograph of the end of the actual spindle with coil. Right: a match by comparison on the same scale.

nous motor is used to drive the coil, the speed then being constant in so far as the mains frequency is constant.

In the instrument under review, the spindle of the small synchronous motor carries an extension piece of some easily machinable plastic such as "Perspex". A very small coil is mounted in this spindle, near the extremity *(fig. 1)*. The A.C. voltage generated when the coil is revolved in a magnetic field, is taken by means of bronze contact rings and silver springs *(fig. 2)* through a screened cable to an amplifier, where the signal is amplified, rectified, and measured by a moving-coil instrument. The deflection of this meter is a direct measure of the field component perpendicular to the spindle at the point where the coil is located. The equipment is shown in use in *fig. 3*.

The exploring coil used in this case is considerably smaller than anything made hitherto for equipment of this type. The inside and outside diameters are 0.5 and 1 mm respectively, and the length is 1.5 mm. These very small dimensions make it possible to measure local values in inhomogeneous fields without difficulty.

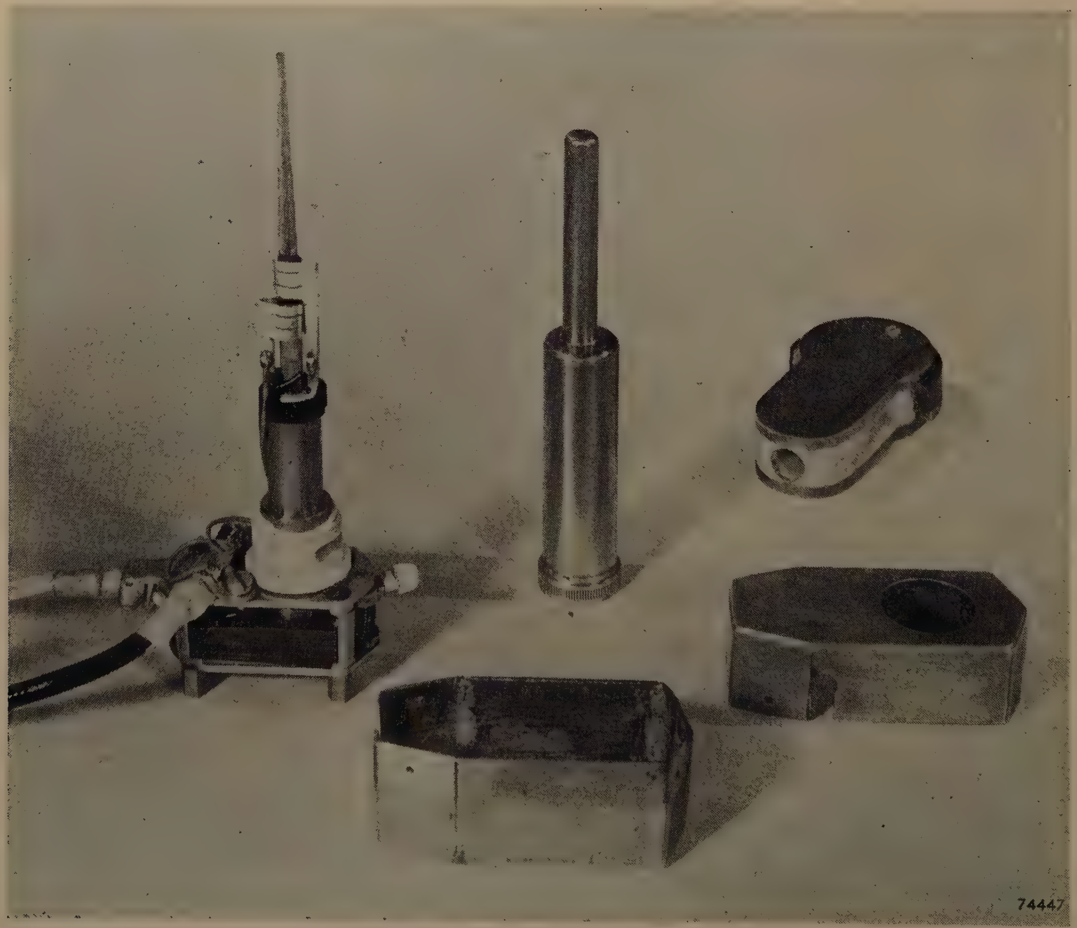

Fig. 2. The synchronous motor with "Perspex" extension piece. The silver contact springs for collecting the voltage can be clearly seen. In addition to the motor housings and the spindle cover, a magnet used for calibration of the instrument is shown in the photograph (background, right).

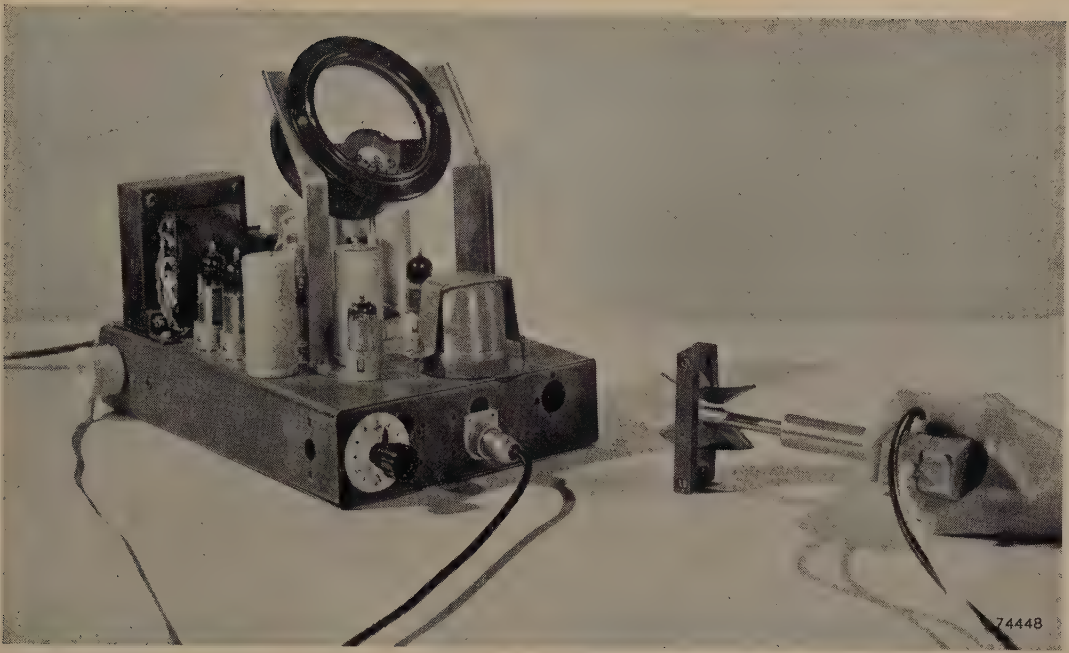

Fig. 3. The field-strength meter in operation. At right: the motor is held in the hand and the exploring coil in its cover is inserted between the pole pieces of the magnet to be measured. At the left is the amplifier and meter.

In such a small coil the flux per turn will of course be very small indeed; moreover, the number of turns cannot be very great, as there is a practical limit beyond which the thickness of the wire cannot be reduced. The sensitivity of the exploring coil drops sharply with the dimensions, but, owing to the amount of amplification provided, the meter gives full scale deflection (at max. amplification) for a field of 3×10^{-4} Wb/m^2 (3 gauss).

The coil is made of enamelled copper wire 25 microns in diameter, which, in the space available permits of 500 turns. With a view to the desired sensitivity a fairly high speed of rotation was adopted, viz. 50 revolutions per second (3000 r.p.m.) It would not be possible to go much beyond that, seeing that no extra bearings are provided for the "Perspex" extension on the motor spindle.

When the rotating probe is held with its axis parallel to the lines of force at the coil, the field component in the plane of rotation is zero and the meter gives no deflection. This, then, is a means of ascertaining the direction of the lines of force. The absolute value of the induction is measured by finding the position corresponding to maximum meter deflection. It is of course necessary that there is sufficient room for such positioning.

In order to ensure optimum transfer of energy from the exploring coil to the amplifier, it is necessary to match the impedance of the former with the input impedance of the latter. This impedance consists almost solely of the attenuator which is provided to permit variation of the measuring range, and is 500 000 Ω (see *fig. 4*). At a frequency of 50 c/s the self-inductance of the exploring coil is still determined only by the D.C. resistance, which is 70 Ω. It was accordingly found desirable to couple the coil to the amplifier by means of an input transformer. Now, the available voltage induced in the exploring coil is divided between the resistance of the coil itself and the inductive impedance of the transformer. When the frequency increases, this inductive impedance rises and, with it, the ratio of the voltage across the primary of the transformer to that induced in the exploring coil. In the region of 50 c/s this ratio is roughly proportional to the frequency [2]). As the voltage induced in the exploring coil itself is also proportional to the frequency (speed of rotation) the potential applied to the grid of the input valve of the amplifier is approximately proportional to the square of the mains frequency. Now, in order to avoid serious errors in measurement arising from this, in the event of fluctuations taking place in the mains frequency, the amplifier was designed to have a response curve such that the gain in the region of 50 c/s decreases as the square of the frequency. For this purpose two *RC* filters are employed, these being located between the first and second amplifier valves (fig. 4).

---

[2]) It is possible to design a transformer which, under the conditions described, will ensure a voltage ratio that is practically independent of frequency in the region of 50 c/s.

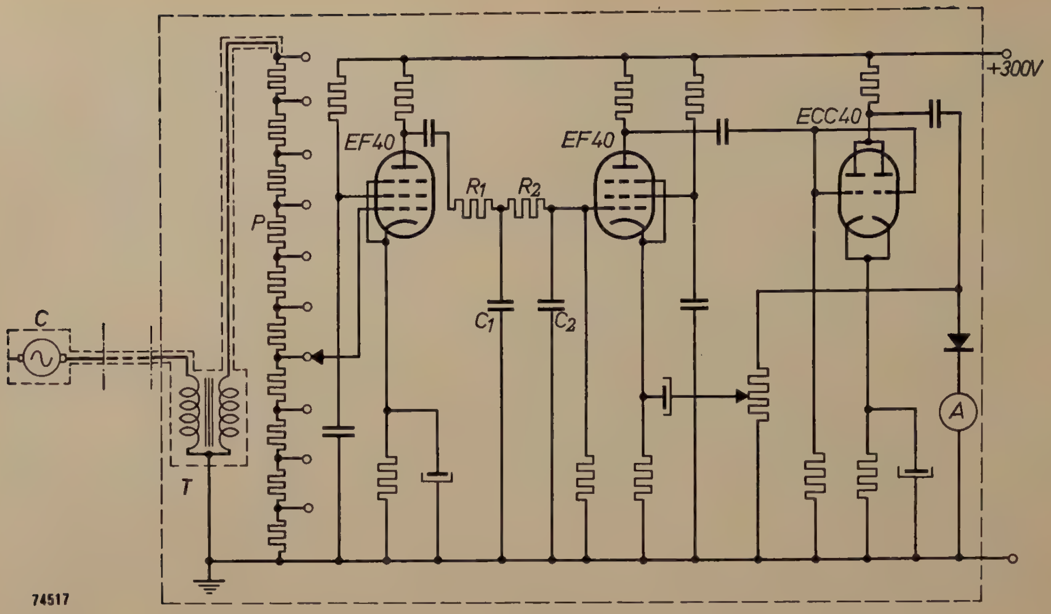

Fig. 4. The amplifier circuit. The voltage generated in the exploring coil *C* is taken across a magnetically screened input transformer *T* to the amplifier. The effect of the double *RC* filter (R_1-C_1 and R_2-C_2) between the first and second valves is to modify the response curve in such a way that the reading will be independent of the mains frequency. *P*, calibrated attenuator for the different measuring ranges. *A*, represents the meter.

The input transformer is provided with effective magnetic screening to avoid interference due to magnetic leakage-fields set up by the mains transformer (such fields are of the same frequency as that of the signals used); the screened transformer can be seen at the front of the chassis shown in fig. 3.

A stabilized supply unit is used for the amplifier, so that variations in the mains voltage shall not affect the amplification.

The complete unit is calibrated by placing the exploring coil in a magnetic field of known strength; the calibrating magnet supplying this field is depicted at the rear in fig. 2. The space between the pole pieces of the magnet is filled with wood in which a hole is provided that just accommodates the screening tube on the "Perspex" spindle. To give the desired reading of the known field strength on the meter, the amplification is adjusted by means of variable feed-back. Since the attenuator has a linear calibration with respect to the meter, the reading is then correct in all the other measuring ranges as well.

In the most sensitive position, a full-scale deflection corresponds to an induction of 3×10^{-4} Wb/m^2 (3 gauss), and in the least sensitive position to 3 Wb/m^2 (30 000 gauss). The error is roughly 3% of full scale, except in the lowest measuring ranges (viz. 3×10^{-4} Wb/m^2 and 10^{-3} Wb/m^2). With such low induction values, a certain amount of interference is experienced in the form of a meter deflection not due to the magnetic field, and corresponding to about 3×10^{-5} Wb/m^2.

II. MEASUREMENT OF THE FIELD ON THE AXIS OF MAGNETIC ELECTRON LENSES

In order to determine the focusing characteristics of magnetic electron lenses such as those used in electron microscopes, it is usually necessary to ascertain the form of the field along the axis of symmetry. When this is known a computation can be made of the field away from the axis.

This statement holds for a part of the space in which no electric currents flow and no magnetic materials occur, and this is the case in the vicinity of the axis of a magnetic electron lens. In such spaces the value of the magnetic induction can be derived from a scalar potential conforming to Laplace's equation. (The derivation is an application of potential theory.)

In essence, a magnetic electron lens consists of a coil enclosed within a soft iron housing (see sketch *fig. 1a)*. The curve representing the field along the axis is more or less bell-shaped. (fig. 1*b*). Approximate computation of this field is possible, but the accuracy is not always high enough for the purpose in view, especially if saturation phenomena occur in the iron. If, say, the spherical aberration of a lens is to be calculated with any precision, the error in the calculation for the field should not exceed 1%. It is better, therefore, to measure the field direct from the lens itself, or from an enlarged or reduced scale model of it.

In the following a description is given of a method of measuring, rapidly and sufficiently accurately, the induction along the axis of a magnetic electron lens. This method is a modified version of the one employed by Van Ments and Le Poole for the same purpose [1]).

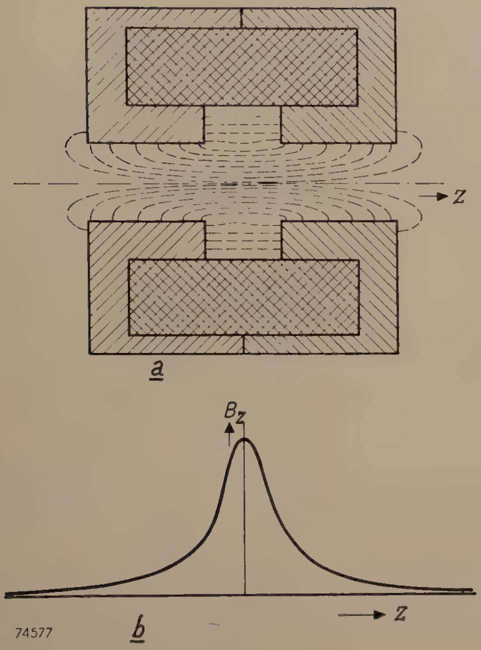

Fig. 1. *a*) Diagrammatic representation of a magnetic electron lens. The lens consists of a coil, almost wholly encased in soft iron; on the inner surface is a small air gap. The field is concentrated mainly inside the coil, near the gap in the iron. *b*) The curve of the magnetic induction B_z on the axis of such a lens is more or less bell-shaped.

Van Ments and Le Pool measured the static force exerted upon an exploring coil within the magnetic field, with a constant direct current flowing through the coil. The coil is specially shaped and consists of a long thin solenoid, the windings of which are reversed at the mid-point M (*fig. 2*). To make the measurement, the coil is positioned with its axis coincident with that of the electron lens. The length of the solenoid is such that the two ends are then situated at points where the field is practically zero.

The principle upon which the measurement is based may be described as follows. Each turn of the coil, as far as its magnetic properties are concerned, may theoretically be replaced by a flat plate, homogeneously magnetized in a direction perpendicular to its face. The plate would have the same thickness and periphery as one turn of wire; one side of it would carry a uniformly distributed positive magnetic charge and the other a similar negative charge, so that adjacent positive and negative charges of the successive plates neutralise each other. At the point where the winding direction changes, however, like charges face, and therefore reinforce each other. Magnetic charges would also occur at the end faces of the solenoid, but these are outside the field and therefore experience no force. The charge at M, on the other hand, encounters a force that is proportional to the induction at that point. The magnitude of the magnetic charge is proportional to the current flowing in the solenoid and, if this current is constant, the force on the solenoid must be a measure of the induction at M.

In fact, the force on the solenoid is not proportional to the induction along the axis at M, but to the flux Φ_M contained per turn at M. If we denote the axial components of the magnetic field strength and the magnetic induction by $H_{\rm ax}$ and $B_{\rm ax}$ respectively, and the (constant) density of the magnetic surface-charge at M by σ, the force on the solenoid will be:

$$K = \int \sigma H_{\rm ax}\,\mathrm{d}S = \frac{\sigma}{\mu_0}\int B_{\rm ax}\,\mathrm{d}S = \frac{\sigma}{\mu_0}\,\Phi_M,$$

where S is the cross-section of the solenoid at M, over which the integration must be performed, and μ_0 is the permeability of a vacuum. Φ_M is of course proportional to the average value of $B_{\rm ax}$ for the cross-section, and what is measured is, in effect, this average.

A correction can be made, however. If we consider the z co-ordinate along the axis of symmetry and denote the flux per turn (radius r) and the magnetic induction on the axis at the point z by Φ_z and B_z respectively, it follows from potential theory that:

$$\Phi_z = \pi r^2 \left\{ B_z - \frac{r^2}{8}\frac{\mathrm{d}^2 B_z}{\mathrm{d}z^2} + \frac{r^4}{192}\frac{\mathrm{d}^4 B_z}{\mathrm{d}z^4} - \dots \right\}.$$

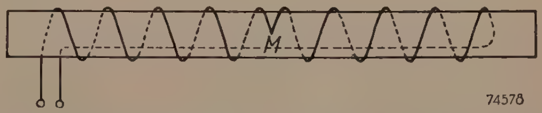

Fig. 2. For the measurement of the field of a magnetic electron lens a long thin solenoid ,the winding direction of which is reversed at the centre M, is used as the actual measuring head. The axis of the solenoid is made to coincide with that of the lens. The force acting on the solenoid is proportional to the magnetic induction at M and to the current flowing in the coil. The ratio of length to thickness is much greater than as shown in the figure.

Here, then, Φ_z is expressed as a series of powers of r. B_z is the term to be evaluated and Φ_z is the value measured. The derivatives $\mathrm{d}^2B_z/\mathrm{d}z^2$ etc., appearing in the corrective terms, are actually unknown, but we can, as an approximation, replace B_z by its average value $\Phi_z/\pi r^2$ for the area of one turn. Then:

$$B_z = \frac{1}{\pi r^2}\left\{ \Phi_z + \frac{1}{8}\frac{\mathrm{d}^2\Phi_z}{\mathrm{d}z^2} r^2 - \frac{1}{192}\frac{\mathrm{d}^4\Phi_z}{\mathrm{d}z^4} r^4 + \dots \right\}. \quad (1)$$

Φ_z is measured as a function of z; hence the derivatives can also be ascertained as a function of z, enabling the corrections to be computed. It will be seen that the corrections are smaller according as r (the radius of the solenoid) is reduced.

---

[1]) M. van Ments and J. B. Le Poole, Numerical computation of the constants of magnetic electron lenses, Appl. sci. Res. **B 1**, 3-17, 1947.

The solenoid can be suspended horizontally on wires (*fig. 3*). When a direct current is passed through it, a deflection occurs owing to the force acting upon it, and this can be measured optically, for example. The deflection is a measure of the induction at the point of reversal in the direction of winding.

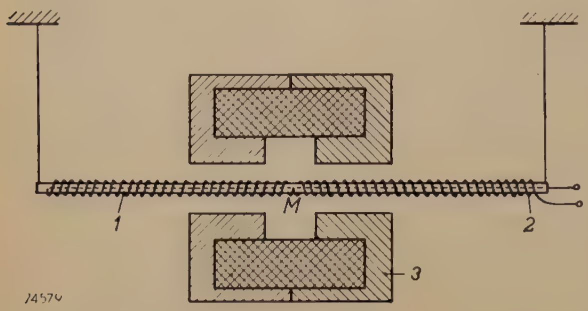

Fig. 3. Principle of system adopted by Van Ments and Le Poole [1]). The rod *1* on which the measuring solenoid *2* is wound, is suspended horizontally by means of thin wires, so as to be concentric with the axis of the electron lens *3*. A horizontal force is exerted on the solenoid in the field of the lens and the resultant displacement, which is measured optically, is a measure of the field strength at *M*.

In the present case, however, another method is adopted; the exploring coil is connected to a source of A.C. voltage, a variable resistor being used to adjust the current flowing in the solenoid to a certain value which is kept constant throughout the process of measurement. The solenoid is thus subjected to a periodic force proportional to the induction at the reversal point in the winding, and accordingly vibrates. The amplitude of this vibration is measured with the aid of an ordinary Philips gramophone pickup of the piezo-electric crystal type. The fact that the signal can be amplified means that measurement is at once simple and accurate.

The solenoid is suspended vertically from two flat springs (*fig. 4*) which also carry a vertical metal plate. This plate follows the vibration of the solenoid. The plate is in contact with the sapphire needle of the pickup and transmits the vibration to the needle by reason of the friction between plate and needle. Should very large amplitudes occur as a result of jarring etc, the needle slips on the plate and damage is prevented. The flat springs and pickup are mounted on a slide in a vertical track which actually forms part of the framework (*9*, fig. 4*a*). To effect the measurement, the electron lens is supported so that its axis coincides with that of the solenoid; the solenoid is then moved vertically along the slide so that the

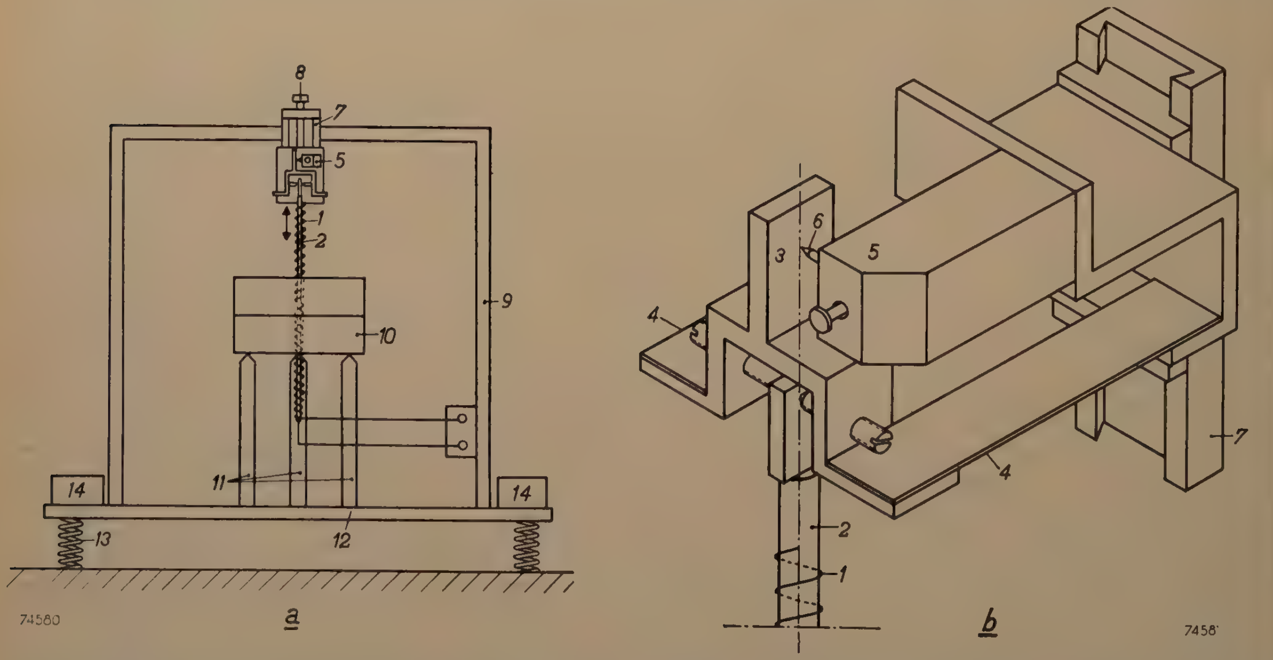

Fig. 4. Schematic view of the system with a vertically suspended solenoid. The coil *1* is wound on an aluminium rod *2* which also serves as return line for the current. An alternating current is passed through the coil, causing this, together with the rod *2* and plate *3*, to vibrate vertically. Vibration is made possible by mounting the system on two horizontal flat springs *4* (see detail in fig. *b*). The amplitude of the vibration is a measure of the magnetic induction to be determined, and is measured by means of a standard Philips gramophone pickup *5*. The sapphire needle *6* of the pickup rests against the vertical plate *3*. For normal measurements, where the amplitude is only a few hundredths of a millimetre, friction causes the needle to follow the motion of the plate. In the event of jarring, the needle slips and damage is avoided. The reversal point in the solenoid winding is positioned at the desired point of measurement by sliding the whole system vertically in a guide *7*; this is effected by means of a screw *8* (not shown in *b*). The guide forms part of the framework *9*. The magnetic lens *10* to be measured is supported on screws *11* for vertical adjustment. Baseplate *12* is mounted on four steel springs *13* to eliminate external vibration, and weights *14* serve to increase the vibration period of the whole system to 0.5 sec.

induction can be measured as a function of the position along the axis of the lens.

Apart from the vibration of the solenoid, the friction plate may very easily transmit undesirable movements to the pickup. e.g. external vibrations originating in the table on which the apparatus is set up. The effect of these vibrations is so marked that its elimination is essential to the effectiveness of the method. The whole apparatus, with the exception of the amplifier and measuring instrument, is therefore placed on a board supported by four vertical compression springs (fig. 4*a*). Weights placed on the plate, moreover, reduce the natural frequency of the whole to about $\nu_0 = 2$ c/s. As the lowest frequencies encountered in floors, walls and tables are usually somewhere between 12 and 20 c/s, the frequencies ν of such extraneous vibrations lie well above ν_0. They are thus transferred to the measuring apparatus attenuated in amplitude [2]) in the ratio $(\nu_0/\nu)^2$. The effect of the external vibration is accordingly reduced by a factor of more than 100.

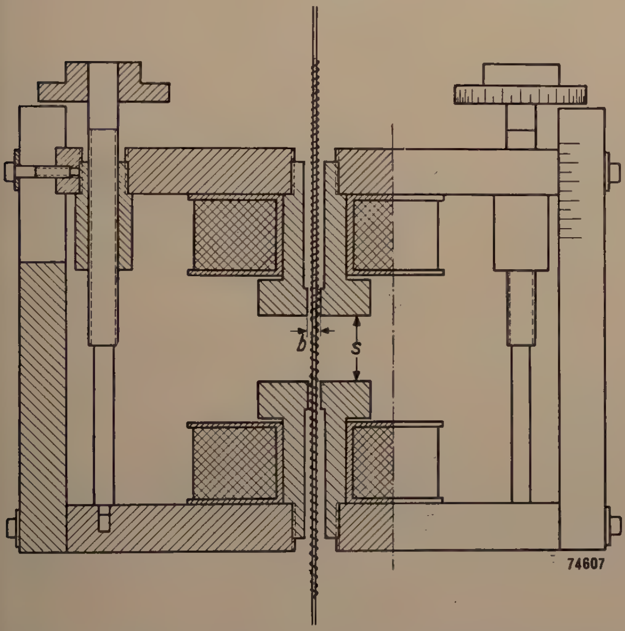

Fig. 5. Magnetic electron lens with bore *b* and variable pole-piece spacing *s*. This lens was specially designed in order to ascertain the effect of the ratio *s*/*b* on the characteristics of the lens. *s*/*b* is variable between 0 and 8.

In the design of electron lenses the dependence of the focusing characteristics on the ratio of pole-spacing *s* to diameter of the bore *b* is of particular interest. A special lens has therefore been constructed,

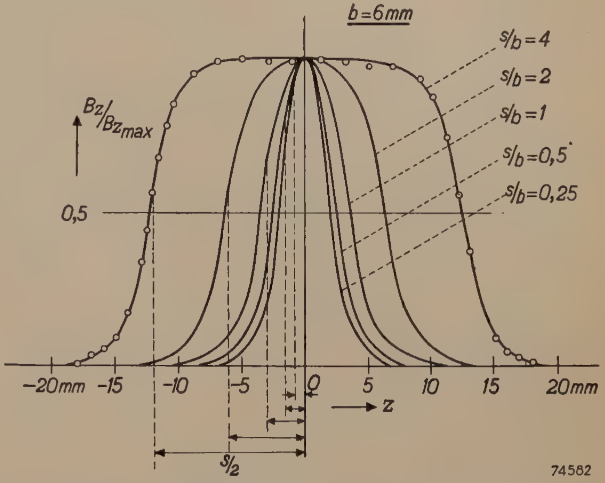

Fig. 6. Results of measurements taken from the lens shown in fig. 5. Relative value of the magnetic induction $B_z/B_{z\max}$ on the axis, for various values of *s*/*b*.

in which the ratio of *s* to *b* is variable between fairly wide limits, viz. 0 to 8 (*fig.* 5). The results of measurements taken from this lens are reproduced in *fig.* 6. These provide a check on the accuracy of the computed values as well as an insight into the effect of saturation in the iron.

The derivatives $\mathrm{d}B_z/\mathrm{d}z$ and $\mathrm{d}^2B_z/\mathrm{d}z^2$, the second of which occurs in the correction terms for B_z in expression (1), can also be measured directly if a small modification be made in the apparatus described above. Instead of the long solenoid, a short coil is placed on an aluminium rod (*2* in fig. 4) suspended from the flat springs. The coil may be visualised as the equivalent of evenly distributed positive and negative magnetic charges at the two end faces of the coil. Since the spacing of these faces is a constant of the apparatus, the resultant force is proportional to $\mathrm{d}B_z/\mathrm{d}z$ at the location of the coil.

If the short coil be made with a reversal of winding direction at the centre, the force to which it is subjected will be proportional to the difference between the forces on the two halves of the coil. The force is thus proportional to the *difference* in the values of $\mathrm{d}B_z/\mathrm{d}z$ for the two halves of the coil and, hence, also proportional to $\mathrm{d}^2B_z/\mathrm{d}z^2$ for the location of the whole coil. In principle it would be possible to measure $\mathrm{d}^3B_z/\mathrm{d}z^3$ with a combination of two divided coils, and so on.

III. MEASUREMENT BY THE PROTON RESONANCE METHOD

The physical principles underlying the two methods already described are so well-known that the emphasis in sections I and II has been on the mode of application rather than on the principles themselves. The third method, however, which is characterized by exceptional accuracy, involves the application of new principles. It is an incidental result of new developments in the sphere of atomic magnetism. A brief outline of these developments will now be given, in so far as they are necessary to an understanding of this method of measurement.

---

[2]) J. A. Haringx, Philips tech. Rev. **9**, 16-23, 1947.

Nuclear spin magnetism and proton resonance

The principle of this method of measurement can be explained broadly and simply in terms of the quantum theory. The proton (nucleus of the hydrogen atom) has a constant mechanical angular-momentum known as the "spin" which is analogous to the spinning of a top. Furthermore, the proton has a constant magnetic moment μ_p. The vectors of the spin and magnetic moment always lie in the same direction, as will be obvious if the proton be imagined as a rotating electrical charge.

According to the quantum theory a proton in a magnetic field B_0 can assume only two orientations, viz. those in which the magnetic moment, and hence also the spin, are parallel, and antiparallel, to B_0. An amount of energy $\Delta E = 2\mu_p B_0$ is needed to change the orientation of a proton from the parallel to the antiparallel position [1]). Thus, spins in the antiparallel position possess an energy which is $2\mu_p B_0$ higher than the energy level of parallel spins. The distribution of the spins among these two energy levels will be in accordance with Boltzmann's law, which states that the concentration in an energy level is proportional to $e^{-E/kT}$, where E is the energy of the level, and k is Boltzmann's constant. The higher the energy the lower the concentration. Let us denote the number of nuclear spins at the lower and higher levels by N_1 and N_2 respectively; then:

$$\frac{N_2}{N_1} = e^{-\Delta E/kT} = e^{-2\mu_p B_0/kT}. \quad . \; . \; . \; . \quad (1)$$

Since, normally, $2\mu_p B_0 \ll kT$, the surplus of protons in the lower level $(N_1 - N_2)$ is very small compared with the total number $(N_1 + N_2)$ of protons [2]).

Suppose that a weak alternating field $B_1 \cos 2\pi\nu t$, of frequency ν be established perpendicular to the field B_0: quantum theory states that energy can be derived from, or imparted to this field only in quantities which are integral multiples of the energy quantum $h\nu$, where h is Planck's constant. If the value of ν is such as will satisfy the equation $h\nu = 2\mu_p B_0$, one single energy quantum will be just enough to change one spin from the parallel to the antiparallel orientation. The chance of parallel spins absorbing energy quanta and becoming antiparallel spins is then greatly increased, i.e., resonance occurs. The frequency at which this takes place is called the resonance frequency ν_r. Hence:

$$B_0 = \frac{h}{2\mu_p}\,\nu_r. \quad . \; . \; . \; . \; . \; . \; . \quad (2)$$

Measuring principle

The above considerations have led to the following method of measuring magnetic fields.

Protons are introduced into the field B_0 to be measured, in the form of hydrogen nuclei from substances rich in hydrogen. A weak alternating field is established perpendicular to the field B_0, the frequency being so adjusted that equation (2) is satisfied. The absorption of energy which occurs at the resonance frequency, is employed as an indicator for the adjustment, and the apparatus therefore includes a cathode-ray oscilloscope, from which the occurrence of this energy absorption can be noted visually. As the resonance frequency is related to B_0 (see eq. 2), the measurement of the magnetic field is now reduced to a measurement of frequency. Since high frequencies can be measured very accurately with little difficulty and, as the onset of resonance is very sharp, this method of measuring magnetic induction is much more precise than other, traditional methods.

For the comparison of magnetic fields it is only necessary to determine the resonance frequencies in these fields. Nevertheless it is also possible to effect absolute measurements, seeing that the exact value of $h/2\mu_p$ is known. With ν_r in cycles per second, we may write:

$$\begin{aligned} B_0 &= 2.3489 \times 10^{-8}\,\nu_r \text{ Wb/m}^2 \\ &= 2.3489 \times 10^{-4}\,\nu_r \text{ gauss.} \quad . \; . \; . \quad (3) \end{aligned}$$

A resonance frequency of 30 Mc/s therefore occurs in a field of 0.7047 Wb/m² = 7047 gauss.

---

[1]) B is written instead of H because of the definition of the magnetic moment. The proton is visualised as a very small circuital current, and the local magnetic field (in vacuo) is defined by the magnetic induction B. The magnetic moment of a plane circuital current i encircling a plane surface S is defined as $m = iS$. The couple imparted to such a circuit in a magnetic field B whose lines of force make an angle ϑ with the normal at S, is $iSB \sin \vartheta$. Sometimes the magnetic moment is defined as $m' = \mu_0 iS = \mu_0 m$. The expression for the resultant couple is then $m'B \sin\vartheta/\mu_0 = m'H \sin\vartheta$. ($H$ = magnetic field strength).
These last expressions for the magnetic moment and resultant couple are automatically arrived at if the magnetic moment be imagined as the outcome of a combination of equal but opposed magnetic charges. We shall, however, adhere to the first-mentioned definition (see for example Slater and Frank, Electromagnetism, McGraw Hill, New York 1947, p. 59).

[2]) $\mu_p = 1.410 \times 10^{-26}$ A.m² and $k = 1.375 \times 10^{-23}$ J/degree. With a field $B_0 = 1$ Wb/m² (10 000 gauss) and a temperature of 300 °K, $2\mu_p B_0/kT \approx 10^{-5}$ and N_2/N_1 is accordingly very little less than unity.

The value of $h/2\mu_p$ can be derived very exactly from measurements taken by Bloch and Jeffries [3]) who set out to determine the value of μ_p, making use of the proton resonance described. The principle on which their measurements were based is as follows. Since protons carry an electric charge e ($e = 1.6019 \times 10^{-19}$ coulombs) they will experience a force when moving in a magnetic field. When the movement is in a plane perpendicular to a *homogeneous* field (B_0, say) they will describe circular paths, which they traverse with a frequency ν_c (independent of velocity) given by:

$$\nu_c = \frac{eB_0}{2\pi M_p} \quad . \quad . \quad . \quad . \quad . \quad . \quad . \quad . \quad . \quad . \quad (4)$$

(M_p = mass of the proton = 1.6722×10^{-27} kg).

Suppose we have a cyclotron with a magnetic field strength B_0; ν_c is then the frequency for the Dee voltage in order that the cyclotron may accelerate protons [4]). Bloch and Jeffries employed a small, specially constructed cyclotron and determined the frequency at which this functioned with protons; this was the frequency ν_c. In the same cyclotron field they then ascertained the proton resonance frequency ν_r which, in accordance with equation (2) is given by:

$$\nu_r = \frac{2\mu_p B_0}{h} \quad . \quad . \quad . \quad . \quad . \quad . \quad . \quad . \quad . \quad . \quad (5)$$

From (4) and (5) it follows that:

$$\frac{h}{2\mu_p} = \frac{\nu_c}{\nu_r} \cdot \frac{2\pi M_p}{e} .$$

The interesting point is that the induction B_0, which cannot be independently determined with any great accuracy, is thus eliminated from the equations. According to the measurements of Bloch and Jeffries, $\nu_r/\nu_c = 2.7924 \pm 0.0002$. Using the above-mentioned values of e and M_p, we find that $h/2\mu_p = 2.3489 \times 10^{-8}$, which value appears in equation (3). (Since h is known, the value of μ_p itself can also be computed.)

Before we proceed to a description of the measuring equipment itself, it is necessary to discuss in greater detail two further points, viz. the magnitude of the energy absorption, and the "line width" of this absorption.

Magnitude of the energy absorption

As already mentioned, there is, in respect of every parallel spin, a certain chance that it will absorb an energy quantum from the field and thus change to the antiparallel orientation. On further consideration, however, this is in itself not enough to explain the energy absorption observed. There is, in effect, an equally good chance that the alternating field may induce a proton with antiparallel spin to release an energy quantum and thus assume the parallel position, this process being known as "induced emission". Both chances are proportional to the concentration of energy quanta of the alternating field, that is, to the energy density of this field, i.e. to B_1^2. Now, the number of parallel spins N_1 is greater than that of the antiparallel N_2 (Boltzmann distribution; equation (1)), so that, from the start, more parallel spins change to antiparallel than vice versa; consequently N_2 increase at the expense of N_1, but, as N_2 and N_1 approach each other, this process slows down. In the absence of any other influences, a situation would finally arise in which $N_2 = N_1$, with just as much energy absorbed from the alternating field as is restored to it; the net absorption would then be zero. Energy absorption would then take place only during such time as N_2 were approaching N_1, and the total absorbed energy would be so small as to be undetectable.

There is, however, another mechanism that causes reversal of the spins, and this is associated with the thermal motion. An interchange of energy occurs between the magnetic energy of the protons in the magnetic field B_0, and the kinetic energy of their thermal motion; this process tends to restore the original Boltzmann distribution (1) of the parallel and antiparallel spins. On average, therefore, the spins release energy towards the thermal motion, and an equilibrium is set up in which the spins take up just as much energy per second from the alternating field as they impart to the thermal motion. If this release of energy is sufficiently great, then, a considerable amount of energy can be absorbed continuously from the alternating field. It is this absorption, as already mentioned, which serves as an indicator for the attainment of the resonance frequency.

The protons, which are brought into a state of resonance in the apparatus about to described, are actually those forming the nuclei of hydrogen atoms in a small quantity of water. With pure water, however, the continuous energy absorption from the alternating field is too small to yield a clear indication, the reason for this being the very slow transfer of the magnetic energy of the protons to the thermal motion. This transfer is enhanced by adding paramagnetic ions to the water, e.g. by dissolving ferric or manganese salts in it. Because of the pronounced interaction between the magnetic fields of the protons and the strong fields of the ions, the exchange of energy is much greater and so also is the amount of energy absorbed from the alternating field. The resonance indication is then clear enough for a practical measurement.

---

[3]) F. Bloch and C. D. Jeffries, A direct determination of the magnetic moment of the proton in nuclear magnetons, Phys. Rev. **80**, 305-306, 1950.

[4]) See for example W. de Groot, Cyclotron and synchro-cyclotron, Philips tech. Rev. **12**, 65-72, 1950.

Line width; sharpness of the resonance indication

The field of the protons and that of the paramagnetic ions, alternating in time and space, are superimposed on the external field B_0; the protons accordingly exist in fields that exhibit a certain variation about the value of the external field B_0. There is therefore not one specific resonance frequency, but a certain range of frequencies in which resonance occurs, and this range lies on and around the frequency corresponding to B_0. The resonance thus possesses a finite "line width". If the rate of absorption of energy, for a constant value of B_0, is plotted as a function of the frequency, the absorption spectrum reveals the peak shown in *fig. 1a,* rather than a clearly defined line at $\nu_r = 2\mu_p B_0/h$ (see Eq. 2). Similarly, when the rate of absorption of energy is plotted against the external field B for constant frequency, a straight absorption line is not obtained for $B = h\nu_r/2\mu_p = B_0$, but again a peak of finite width about B_0 (fig. 1*b*). According to whether we are considering fig. 1*a* or 1*b*, the line width can be expressed in c/s or Wb/m². The relationship between the two alternatives follows at once from equation (3): 1 c/s corresponds to 2.3489×10^{-8} Wb/m².

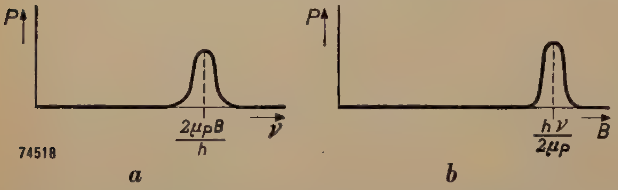

Fig. 1. "Line width" of proton resonance in a magnetic field B with a superposed perpendicular H.F. field (frequency ν). Resonance can be attained in two ways, viz. 1) with constant external field B, by varying the frequency of the H.F. field; 2) with constant frequency, by varying the external field B. For measuring purposes the two methods are combined.
a) With constant external field B, resonance occurs in a small range of frequencies about the frequency value relevant to the field B, in accordance with equation (2). P is the absorbed power.
b) With constant frequency, resonance occurs in a range of magnetic induction values about the value relevant to that frequency, in accordance with equation (2). The line width can therefore also be expressed in Wb/m².

For pure water the line width is roughly 10^{-6} Wb/m² (10^{-2} gauss). The addition of paramagnetic ions increases the width, as is to be expected, since the magnetic fields of these ions increase the "spread" of the local fields around the value of B_0. At the same time, even when pure water is replaced by a solution of ferric or manganese salts, the line remains so narrow (in our case 10^{-5} Wb/m² = 0.1 gauss) that the definition of the resonance indication is not appreciably affected. These figures demonstrate the sharpness of the resonance indication. The inhomogeneity of strong magnetic fields (of the order of 1 Wb/m²) within the space occupied by the measuring head (about 30 mm³), even in the most uniform fields, is usually of the same order of magnitude, so that greater precision in the indication of resonance would in any case be superfluous.

Description of the proton resonance equipment

The equipment about to described was constructed along the lines of a design previously employed by Pound and Knight [5]). A coil, wound round a small "Perspex" container, is contained in a flat coil-holder (*fig. 2*), the axis of the coil lying in the plane of the holder. The holder is inserted in the magnetic field to be measured with its flat face at right angles to the lines of force. An alternating current passed through the coil produces the weak alternating field perpendicular to the field to be measured. The "Perspex" chamber is filled with an aqueous solution of manganese sulphate or ferric nitrate, to provide a certain concentration of manganese or ferric ions. The hydrogen atoms of the water

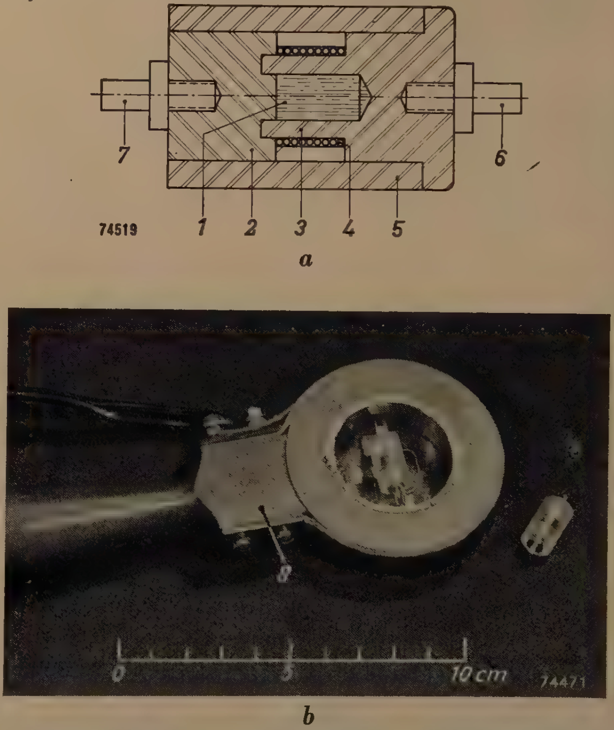

Fig. 2. *a*) Construction of the oscillator coil. The cavity *1* (internal diam. 3 mm, length 4 mm) contains a solution of a ferric or manganese salt. The walls are formed by the "Perspex" components *2* and *3*. *4* is the oscillator coil proper. *5* is a "Perspex" bush. *6* and *7* are brass terminals for the coil.
b) The oscillator coil is fitted in the centre of a flat coil holder *8*. The lead for connection to the capacitor in the oscillator circuit is taken through the handle of the holder; on the left will be seen leads for an auxiliary coil which produces a ripple on the field to be measured. At right: oscillator coil for a different measuring range.

---

[5]) R. V. Pound and W. D. Knight, A radio frequency spectrograph and magnetic field meter, Rev. sci. Instr. **21**, 219-225, 1950.

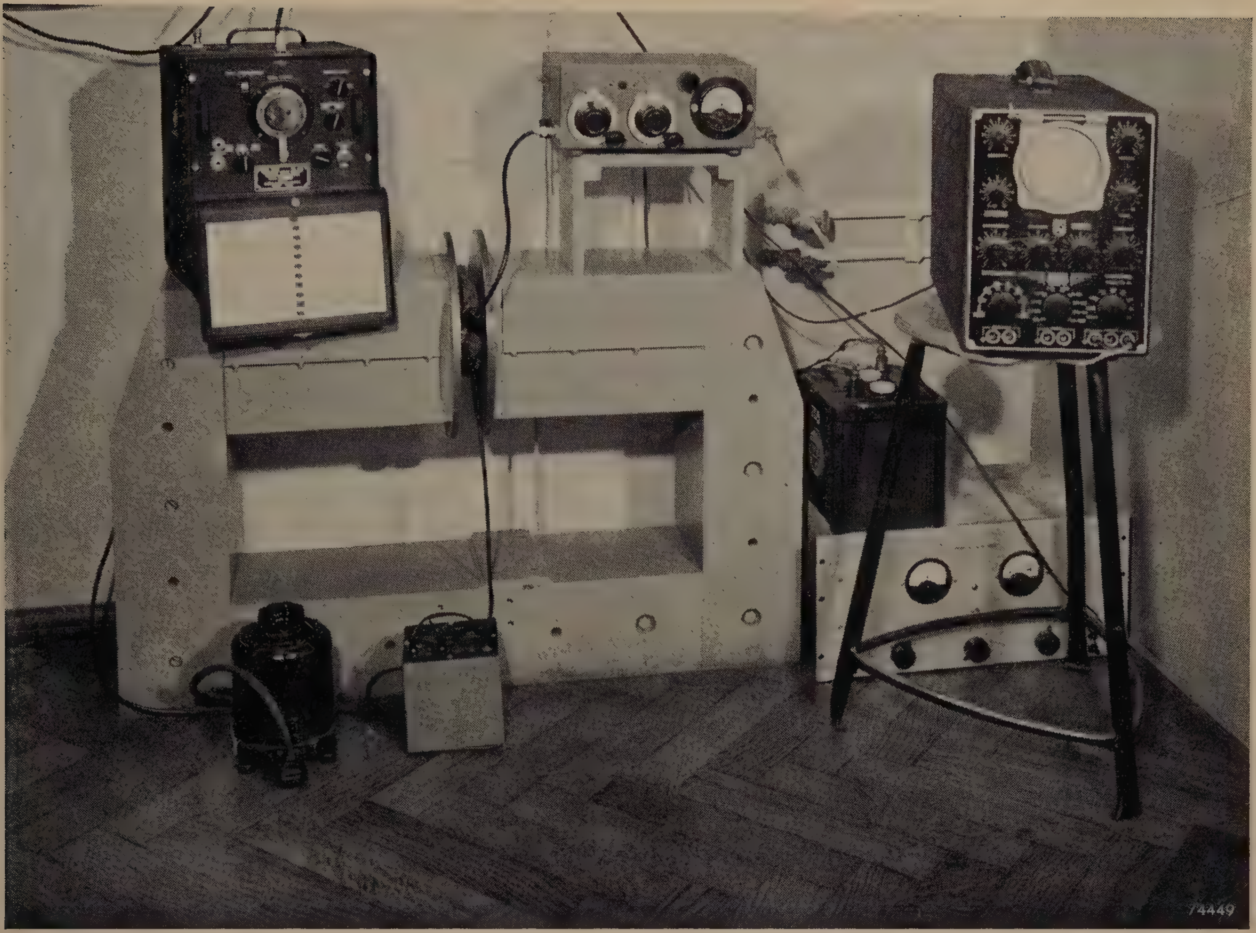

Fig. 3. Measuring the magnetic field of a large permanent magnet (weight 600 kg) by means of the proton resonance equipment. The coil holder is inserted between the pole pieces of the magnet. The electronic equipment is standing on the right-hand pole piece; on the right of the illustration is the oscilloscope for the resonance indication. At right below, high tension unit and battery supplying heater current for the valves. Standing on the left hand pole piece of the magnet is the wavemeter used for measuring the resonance frequency. On the ground at left: a variable transformer to supply the ripple added to the measured magnetic field.

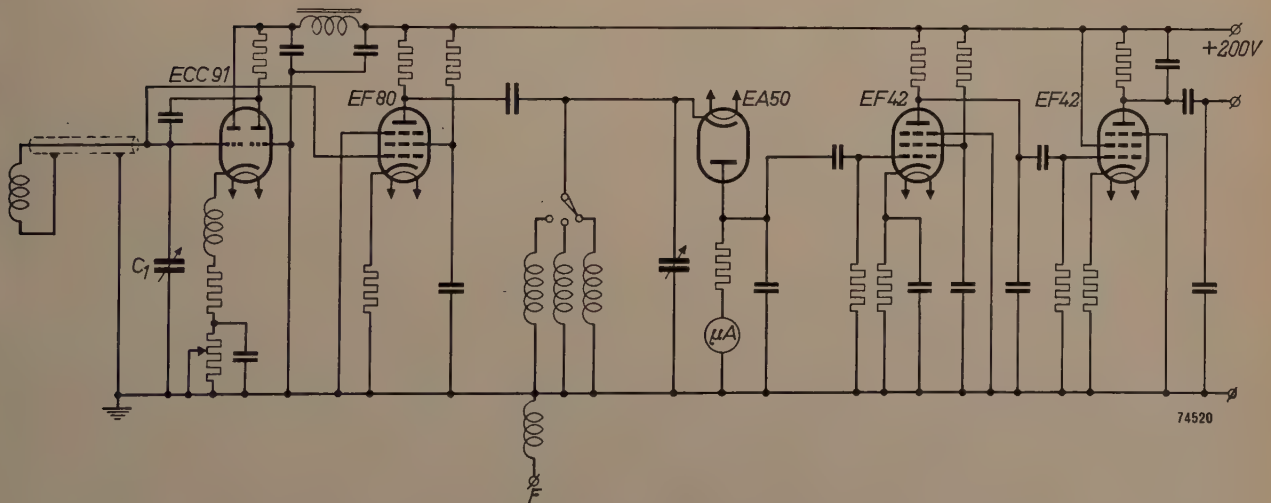

Fig. 4. Circuit diagram of the proton resonance measuring equipment. On the left is the exploring coil connected to capacitor C_1, and a double triode operated as negative resistance to form an oscillator. On the right-hand side of this valve is the circuit for amplification and detection of the voltage modulation in the oscillator circuit. *F* connecting point for wavemeter.

contain the protons which are to be brought into resonance in the measured field, and the paramagnetic manganese or ferric ions ensure an effective transfer of the energy absorbed at resonance to the thermal motion.

A low-capacitance coaxial cable connects the coil to the electronic equipment (*fig. 3*). The coil, together with a capacitor C_1 and the cable capacitance, constitute a tuneable oscillator circuit (*fig. 4*); this is coupled to a negative resistance circuit formed by a double triode ECC 91 to complete the oscillator circuit. The frequency of this circuit is tuned to the resonance frequency of the protons by adjusting C_1. In order to cover a wide frequency range, the coil is interchangeable (fig. 2). There are in all three coils, each with a different number of turns.

By means of the biasing resistor common to the two triodes, the oscillator is adjusted to the threshold of oscillation. Under these conditions the voltage on the circuit is very sensitive to the small increase in damping that occurs with proton resonance. In the rim of the coil-holder there is a flat auxiliary coil, through which a 50 c/s current is passed during measurement; this causes the field at the location of the exploring coil to alternate between $B_0 + B_s$ and $B_0 - B_s$. B_0 represents the value of the field to be measured and B_s the amplitude of the field of the auxiliary coil, at the "Perspex" container. Proton resonance and the accompanying absorption of energy will occur twice per cycle of 1/50 sec when the oscillator is tuned to a frequency ν such that (see *fig. 5*):

$$B_0 + B_s \geq \frac{h\nu}{2\mu_p} \geq B_0 - B_s.$$

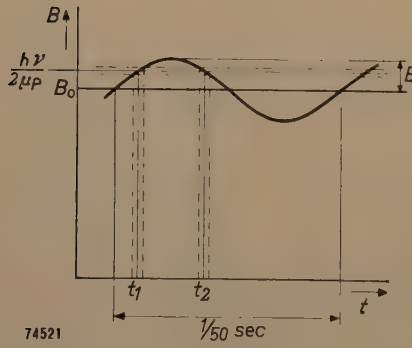

Fig. 5. The auxiliary coil in the coil holder superimposes a ripple of amplitude B_s on the measured field B_0. At a given frequency ν of the H.F. field, resonance occurs when the value of B lies between the two dotted horizontal lines. This occurs twice per cycle of 1/50 sec., viz. about the times t_1 and t_2. The oscilloscope thus reveals absorption peaks at the points corresponding to these times. If, now, the ripple amplitude is reduced under the conditions as shown, where $h\nu/2\mu_p > B_0$, t_1 and t_2 move towards each other. The oscilloscope shows the absorption peaks approaching each other, coinciding and disappearing.

Twice per cycle, then, the resonance requirement $\nu = 2\mu_p B/h = \nu_r$ (see Eq. 2) will be met, and at these moments (t_1 and t_2 in fig. 5), the voltage of the oscillator circuit will vary by a small amount. Owing to the finite width of the resonance range (shown by the horizontal dotted lines), the instants of time are increased to short time intervals. The high-frequency signal across the circuit is modulated by these dips in voltage. The fundamental frequency of the modulation is thus 50 c/s.

The signal is first amplified by an EF 80 valve, the anode circuit of which is tuned by means of a variable capacitor and one of three coils operated by a switch, corresponding to the exploring coil used in the coil holder. Next the signal is rectified and smoothed by a combination of capacitor and resistor with low time constant, to avoid attenuation of the peaks, which occurs with a frequency of 50 c/s. Finally, the signal, which now contains only the absorption peaks, is again amplified and applied to a cathode-ray oscilloscope. The time base is synchronised with the 50 c/s voltage on the auxiliary coil. When resonance conditions are obtained, two absorption peaks are seen on the screen, well above the noise level (*fig. 6* shows two pairs of peaks, this being due to the use of a 25 c/s time base).

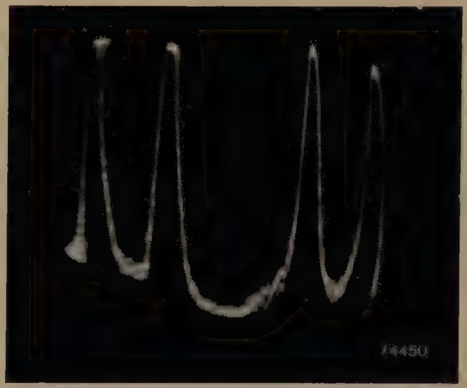

Fig. 6. Oscillogram of modulation of the oscillator amplitude. The frequency of the time base in this case was 25 c/s: hence the two pairs of peaks.

To measure a magnetic field B_0, the current in the auxiliary coil is gradually reduced. In the case of fig. 5, when the frequency is too high, the traces of the two peaks will be seen to come together, coincide and then disappear; when the frequency attains the value $\nu_r = 2\mu_p B_0/h$ appropriate to B_0, the peaks remain stationary (*fig. 7*). (Because of the finite width of the resonance zone, the peaks become wider according as B_s is reduced. When the ripple on B_0 lies wholly within the resonance zone, the resonance is continuous and, with it, the absorption, in which case the H.F. voltage on the oscillator circuit is no longer modulated, but has a constant value. As only the modulation is visible, the peaks then disappear from the screen.) The resonance adjustment, then, consists of tuning the oscillator till the separation of the peaks becomes insensitive to changing the current in the auxiliary coil. The frequency is then carefully measured, e.g. by means of a calibrated auxiliary oscillator beating with the signal. Finally, the value of the field is obtained with the aid of equation (3).

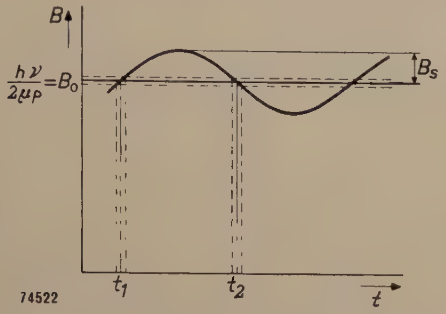

Fig. 7. The frequency ν being so adjusted that $h\nu/2\mu_p = B_0$, the absorption peaks remain stationary when the ripple amplitude is reduced. This is the indication that the frequency is correct.

With little trouble the frequency can be measured with a relative error of less than 10^{-4} but, if a smaller accuracy is sufficient, use can be made of a previously prepared chart showing the frequency plotted as a function of the reading of the capacitor C_1.

The amplitude of the alternating field

One or two points will now be mentioned concerning the choice of amplitude B_1 of the high-frequency alternating field. Any increase in B_1 results in an increase in the concentration of energy in this field, and more energy quanta are then available for raising protons to the higher energy level. In the resultant new condition of equilibrium, the difference in the concentration of the two possible levels would then be smaller, which means that the departure from the Boltzmann distribution would be greater and the release of energy to the thermal motion accordingly increased. Since this release of energy is equal to the absorption of energy from the alternating field, the absorption will likewise increase. It will be clear, however, that, according as B_1 is increased further, the departure from the Boltzmann distribution approaches a limit, viz. the point corresponding to equal concentrations in the two energy levels (see page 57). Simultaneously the release of energy to the thermal motion would also approach a limiting value, with a corresponding limit to the energy absorption from the alternating field. An indefinite increase in the absorption peaks seen on the oscilloscope cannot therefore be expected as B_1 is increased. In practice it is observed that while the peaks first increase in size, they subsequently *collapse* with further increase in B_1. That this must be so is easily demonstrated. In the description of the equipment it was mentioned that the oscillator must be adjusted to the threshold of oscillation, as it is then most sensitive to variations in the damping. In order to increase B_1 the oscillator must be made to oscillate more strongly and the sensitivity to variations in the damping then drops; the increase in damping and the drop in sensitivity thus counteract each other. When the absorption approaches its maximum value, the decrease in sensitivity gains the upper hand and the absorption peaks shrink in size.

Classical considerations

Mention should be made of the fact that the subject of proton resonance can be viewed in the light of the laws of classical mechanics [6]). This is a fairly complicated procedure however and gives a less straightforward picture than the simplified explanations given here on the basis of the quantum theory. In the classical theory the proton is regarded as a kind of top, which executes a precessional motion under the influence of magnetic fields [7]). The transfer of energy to the thermal motion takes place with a certain delay which is expressed as a certain relaxation time. This relaxation time is considerably reduced by the addition of paramagnetic ions.

Apparatus for fields up to 1.4 Wb/m² (14 000 gauss)

The measuring range of the equipment described above is roughly 0.16 to 0.82 Wb/m² (1600 to 8200 gauss), corresponding to a frequency range for the oscillator of 6.8 to 35 Mc/s. Another unit has now been made up, which measures field strengths up to 1.4 Wb/m² (14,000 gauss) (*fig. 8*). The oscillator

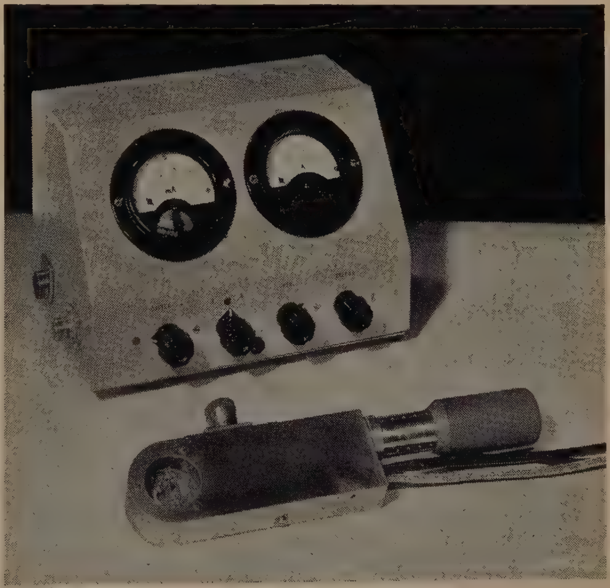

Fig. 8. The proton resonance measuring unit for fields of from 0.5 to 1.4 Wb/m² (5000 to 14 000 gauss). The oscillator frequency is variable from 21 to 60 Mc/s, this being possible because the whole oscillator is housed in the coil holder, thus eliminating the capacitance of the cable between valve and oscillator coil. The double triode is in the handle, that is, as far as possible from the magnetic field to be measured. In strong magnetic fields the triodes will not function. Behind the coil holder will be seen the unit for amplification and detection of the signal. (The lead from the coil holder is shown disconnected.)

---

[6]) F. Bloch, Nuclear induction, Phys. Rev. **70**, 460-485, 1946.

[7]) See also H. G. Beljers and J. L. Snoek, Gyromagnetic phenomena occurring with ferrites, Philips tech. Rev. **11**, 313-322, 1950.

frequency range in this case is extended to 60 Mc/s, this having been made possible by mounting the whole oscillator in the coil holder. This dispenses with the lead between the coil and the oscillator valve, with a corresponding reduction in the circuit capacitance. It is probable that at the upper limit the measuring range could be extended to 2.0 Wb/m^2 (20 000 gauss). A unit for lower field strengths (lower limit approximately 10^{-2} Wb/m^2 (100 gauss) is now in course of development.

Applications of the method

The apparatus described — which is also very suitable for demonstrating the phenomenon of nuclear spin resonance — can be used for checking the variation of induction between the poles of permanent magnets during the course of time. It is also useful for ascertaining the effect of certain external influences such as mechanical impact or vibration of the magnet, temperature variation and so on. As an example, the table below gives details of the field strength at the centre between the pole pieces of a large permanent magnet of "Ticonal" (see Fig. 3). This magnet was fabricated in the Philips laboratories and is used mainly for calibrating coils for fluxmeters.

Table. Induction between poles of large "Ticonal" magnet.

Date	Treatment	Induction in Wb/m^2 as measured after treatment
25-11-51		0.4351
3-12-51		0.4350
16-1-52		0.43325
16-1-52	Heating from 20 to 49 °C	0.4301
16-1-52	Cooling down to 19 °C	0.4326
18-1-52		0.4326
18-1-52	Heating from 20 to 68 °C	0.4284
18-1-52	Cooling down to 20 °C	0.4325

From the measurements it is apparent that a rising temperature cycle results in a drop in the induction, at least, when this occurs for the first time; this process may be regarded as a sort of ageing. It appears from both the temperature cycles that the temperature coefficient of the magnet is roughly 0.85×10^{-4} Wb/m^2 per °C.

Summary of I, II and III. Three instruments for the measurement of magnetic fields, based on three entirely different principles, are described. The first of these makes use of an extremely small coil (outside diam. 1 mm, length 1.5 mm), mounted on the shaft of a small synchronous motor and rotated with constant angular velocity in the field to be measured. The voltage generated is collected by contact rings and springs and is taken to an amplifier and then rectified. The resultant D.C. voltage is a measure of the magnetic induction. The influence of the mains frequency on the induced signal voltage is compensated by a suitable response curve of the amplifier. The measuring range is very wide, viz. 10^{-4} to 3 Wb/m^2 (1 to 30,000 gauss), and the accuracy is 3%.

The second instrument was developed especially for the measurement of fields along the axis of magnetic electron lenses. A long thin solenoid, the winding direction of which is reversed at the centre, is suspended vertically by two flat springs and is mounted so as to coincide with the axis of the electron lens. When a constant 50-cycle alternating current is passed through the solenoid, an alternating force acts upon the coil, this being proportional to the magnetic induction at the point where the winding changes direction. In consequence, the solenoid vibrates vertically, and this vibration is communicated to the sapphire needle of a gramophone pickup. The A.C. voltage thus obtained, which is amplified, is a measure of the induction. In practice, it is essential that the apparatus be so mounted as to be free from external vibration. By this method the field at any point on the axis of a magnetic electron lens can be measured simply and quickly with an error of less than 1%.

In the third method, a small container of water is placed in the field to be measured. A weak alternating field set up at right angles to this field, brings the hydrogen nuclei of the water molecules into resonance. The frequency at which this proton resonance occurs is proportional to the strength of the field to be measured (30 Mc/s in a field of 0.7047 Wb/m^2). Measurement of the magnetic induction is thus reduced to measurement of this resonance frequency, which can be carried out with a high degree of accuracy. The method is very suitable for the accurate, absolute measurement of strong homogeneous magnetic fields (error less than 0.01 %). The measuring range is 0.16 to 0.82 Wb/m^2. Another model has a range of 0.5 to 1.4 Wb/m^2. This method has been employed in the Philips laboratories at Eindhoven to check the stability of a large permanent magnet used for calibration purposes.

THE EFFICIENCY OF FLUORESCENCE IN CATHODE-RAY TUBES

by A. BRIL and H. A. KLASENS.

535.376: 621.385.832

In the manufacture of cathode-ray tubes it is desirable to have quantitative data on the fluorescent efficiency of the screen, i.e. the efficiency of conversion of electron energy to luminous energy. Special measurements and theoretical considerations make it possible to determine the conditions for optimum screen brightness with a given electron energy, in particular for screens coated with a layer of aluminium.

Introduction

The fact that certain minerals fluoresce when subjected to an electrical discharge in a rarefied gas was noted by E. Becquerel about 1860. After the discovery and subsequent study of cathode rays by Hittorf (1869) and Crookes (1879), a special investigation of this kind of fluorescence was made by the latter in such substances as CaS, BaS, diamond, ruby etc. Lecoq de Boisbaudran (1883) made considerable additions to the list of substances that exhibit this phenomenon, which became known as cathodoluminescence.

Lenard (1903), who had done a great deal of pioneer work in the fields of both cathode rays and luminescence, carried out a quantitative investigation into the phenomenon of cathodoluminescence. According to him, the relationship between the brightness L of a screen exposed to cathode rays (electrons), the current density j and the acceleration voltage U, can be formulated as:

$$L = kj(U - U_0) \quad \ldots \ldots \quad (1)$$

where k and U_0 are constants which differ between one case and another. The quantity U_0, i.e. the value of the acceleration voltage below which no noticeable light appears, was given as 300 V for the phosphor CaS-Bi, 1700 V for ZnS and 6000 V for uranium glass.

Other research workers have since carried out more accurate investigations into cathodoluminescence at low acceleration voltages[1]) and have arrived at formulae of the following kind:

$$L = k'jU^n \quad (n > 1) \quad \ldots \ldots \quad (2)$$

The efficiency η of the luminescence, i.e., the ratio the radiation emitted per unit area of the screen to the energy per unit area of the electron beam, jU, is thus defined by the equation $\eta = k''U^{n-1}$.

It will be clear that a formula such as this, in which the efficiency increases steadily with U, can be valid only for a limited range of values of U, since η can of course never be > 1.

The efficiency of cathodoluminescence is nowadays of great practical importance in many technical applications — e.g. for oscilloscopes, television tubes, electron microscopes, radar. Renewed investigations in this field have therefore been made in the Philips Laboratories at Eindhoven. The work was undertaken with a view to obtaining results of practical value but having also a sufficient generality to enable them to be applied independent of arbitrary factors such as the grain size of the phosphor or the thickness of the screen.

The mechanism of cathodoluminescence; conditions for measurement of efficiency

The screen of a cathode-ray tube is usually built up of one or more layers of crystals. With ZnS, for example, the size of the crystal may vary between one and some tens of microns; other substances such as willemite (Zn_2SiO_4—Mn) have smaller crystals. When a crystal of this kind is struck by an electron, the electron may leave the crystal without loss of energy (elastic collision); more frequently, however, the electron will impart some, or the whole, of its energy to the crystal (inelastic collision) and the energy thus released is transferred mainly to the electrons present in the crystal. Within the crystal, then, a swarm of "excited" electrons is formed, which possess extra energy of the order of 10 eV. These excited or secondary electrons will, if the substance is not a "phosphor", ultimately yield up this energy to the crystal lattice without radiation, in the form of heat. With phosphors, on the other hand, some of the excited electrons transfer their extra energy directly or indirectly to so-called luminescence centres, which can then emit a quantum of light[2]). Other secondary electrons will leave the crystal immediately (secondary emission), and this is important from the point of view of the charging of the screen.

---

[1]) For details and bibliography, notably for the period since 1925 see A. Bril and H. A. Klasens, Philips Res. Rep. 7, 401-420, 1952 (No. 6).

[2]) See also A. Bril and F. A. Kröger. Saturation of fluorescence in television tubes. Philips Tech. Rev. 12, 120-128, 1950 (No. 4).

The physicist is interested in all the elements of this process i.e. the number and velocity-distribution of the secondary electrons and the distribution of the radiative and non-radiative energy released in the crystal. Technically, however, the number of emitted light-quanta per primary electron is the main interest. The object of the measurements described in this article and dealt with in greater detail in the article referred to in footnote [1]) is to determine this last-mentioned quantity as accurately as possible.

It has been pointed out that, according to the earlier findings of Lenard as well as to later measurements, the efficiency of cathodoluminescence at low values of the electron energy is very low, but that it rises sharply when the energy is increased. This has been attributed to the small depth of penetration of the electrons when their energy is low. These electrons are for the greater part slowed down in the outer atomic layers of the crystal where, in consequence of lattice defects or impurities, they produce but little luminescence.

To obtain quantitative results which are independent of such surface effects, the investigation of these phenomena is restricted to high electron velocities, corresponding for example to acceleration potentials of 10 to 50 kV. This range of potentials, whereby electrons will penetrate crystals such as ZnS to a depth of 1 to 25 μ, is also the most interesting from the point of view of technical applications.

To yield reliable data of practical value it is desirable that measurements be made with on a comparatively thick phosphor layer (e.g. 0.3 mm). The reason for this is as follows.

As already mentioned, the screen of a cathode-ray tube usually consists of one or more layers of crystals. Consider first a single crystal. Secondary electrons are produced along the path of the primary electrons within the crystal, and some of these secondaries will be responsible for the emission of light. Before the light finally leaves the crystal it will generally be internally reflected a number of times from the faces of the crystal (total reflection), so that the whole crystal, as it were, is filled with light. Hence the crystal may be regarded as a light source, embedded in the screen and emitting light in all directions. Once the light has left the crystal it falls upon neighbouring crystals, which also produce internal reflections and thus pass the light in turn to others. This transfer of the radiation from crystal to crystal is a cause of scattering of the light in the screen which, in itself, does not represent a loss of energy. Apart from the scattering, however, absorption takes place during the passage of the light through the crystals, and this of course is accompanied by a loss of energy.

Consider now the light emitted from both sides of the screen. The two sides do not emit equal quantities of light, the distribution of the total available luminous energy between the two being determined mainly by the scatter and the absorption. These two factors of course depend on the thickness and nature of the screen (crystal size and absorption of the phosphor), as well as on the penetration depth of the primary electrons. If the thickness of the screen be increased, no light will ultimately penetrate to the front of the screen (i.e. the side remote from the electron beam); apart from absorption, all the light will then be emitted from the rear face. This situation would obviously be of little use for practical purposes, but it does lend itself admirably to measurements of the efficiency of the fluorescence.

The measurements are carried out as follows. A beam of electrons of constant current density is allowed to strike a thick screen from a certain angle and the flux emitted per unit area and per unit solid angle is recorded. Since it is permissible to assume that the radiation from a thick screen conforms to Lambert's law (brightness independent of the direction of observation of the screen), it is only necessary to multiply by π the measured specific flux emitted in the direction of the normal in order to obtain the total energy per unit area. If we now divide this by the product of current density and acceleration voltage, that is, by the power per unit area of the primary electron beam, we shall know the efficiency. This efficiency value is to a certain extent influenced by the absorption losses and, if necessary, a correction may be made, based on the fact that the light is actually produced by a very thin surface layer of the phosphor. One half of this light is emitted directly from the back of the screen without appreciable absorption, and the remainder only after diffusion in the phosphor crystals. Owing to absorption, this remainder undergoes a reduction corresponding to the reflectivity R_∞ of an infinitely thick layer of crystals. If we denote the measured efficiency by η_{m}, and the efficiency thus corrected for absorption losses — i.e. the "intrinsic" efficiency — by η_{i}, it follows that:

$$\eta_{\mathrm{m}} = ({}^1/_2 + {}^1/_2\, R_\infty)\, \eta_{\mathrm{i}} \quad . \quad . \quad . \quad . \quad (3)$$

or:

$$\eta_{\mathrm{i}} = \frac{2}{1+R_\infty}\,\eta_{\mathrm{m}} . \quad . \quad . \quad . \quad . \quad (4)$$

The measuring equipment

The apparatus consisted of a demountable cathode-ray tube permanently connected to an oil diffusion pump backed by a rotary oil pump. This tube (*fig.* 1 *a* and *b*) comprises 3 sections, *A*, *B* and *C*. Section *A*, which is of the same design as that used in the Philips' electron microscope, contains the electron gun with an oxide cathode *f* having a core of nichrome wire; this cathode is enclosed in a cap *g* having in it an aperture through which the electrons stream. The space between the cap *g* and the hollow anode *h*, which is attached to the metal wall of *A*, is adjustable. The anode and the shield *A* are earthed, whereas the heater *f* and the cap *g* can be given a high negative potential by means of a transformer and rectifier, this potential being varied from the primary side of the transformer. The leads to the cathode are taken into the tube through a porcelain insulator.

Section *C* is a metal cylinder in which an aluminium plate *P* is mounted at an angle of 45°; this plate has in it a number of shallow recesses which can be filled with various phosphors. The plate can slide along the axis of the cylinder, so that the various phosphors in turn can be subjected to electronic bombardment under identical conditions. The fluorescent radiation is observed, and measured, perpendicular to the plane *P*, through a quartz window *a*. Window *d* serves for the measurement, if desired, of the light emitted from the front of a screen; in this case the solid plate *P* is replaced by a plate with openings carrying glass plates with the phosphors applied to them. Windows *b*, *c* and *e* enable the phosphors to be observed during measurement; in particular, window *b* can also be used for measuring the fluorescent light from directions other than the normal, and also for determining its spectral composition.

A focusing coil *F* is used for concentrating the electron beam on a particular point of the test plate, and two deflection coils *D* enable a limited area of the layer of phosphor (1.5 × 2 cm) to be scanned in two perpendicular directions through this point. In this way the electron beam can be made to trace a raster on plate *P*, this being visible through window *a*. The beam current density is obviously higher than the average current density on the screen. There is some risk, especially

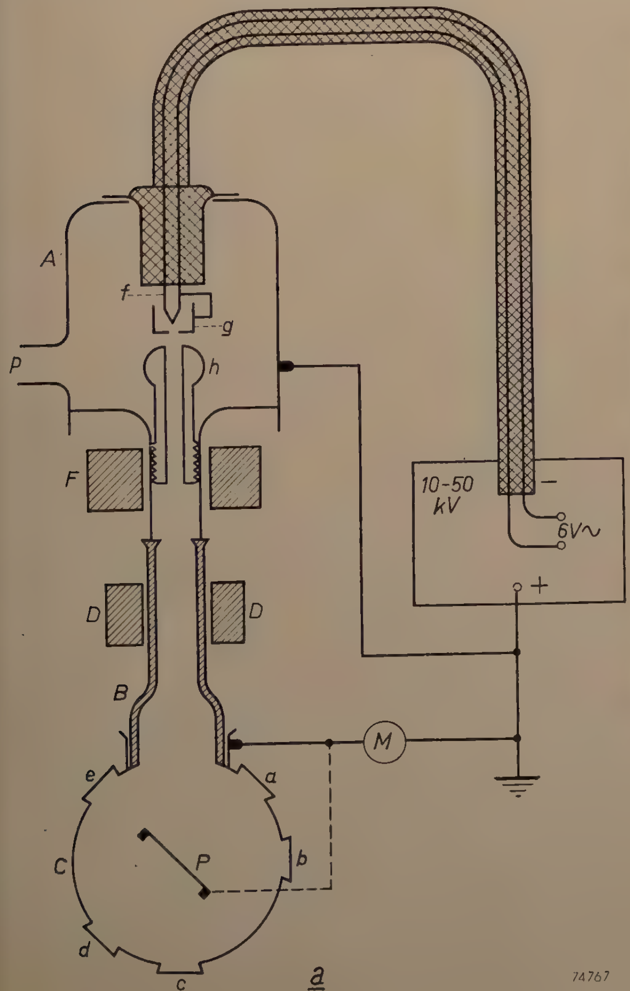

a

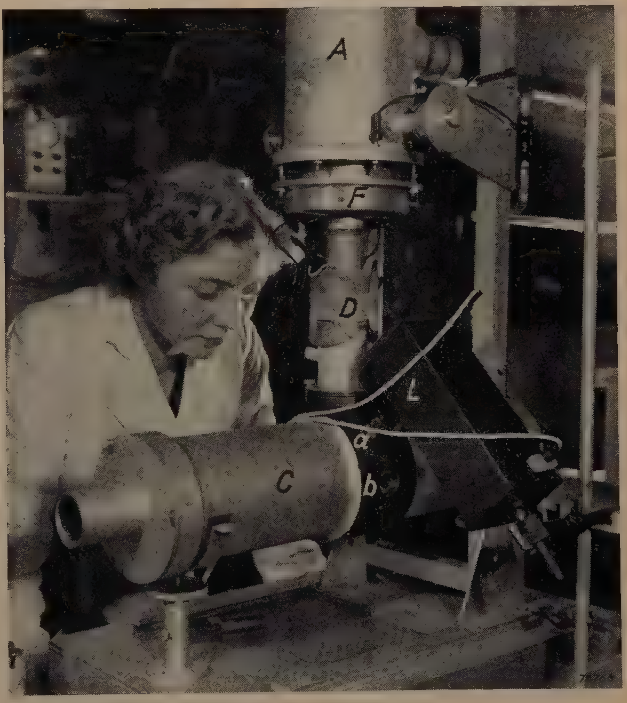

b

Fig. 1 *a*) Diagram of apparatus for the measurement of fluorescent efficiency. *A* metal chamber, *h* anode, *f* filament, *g* cap, *p* pump connection, *F* focusing coil, *D* deflection coils, *B* glass tube, *C* metal cylinder, *P* target plate, *a*, *b*, *c* and *d* quartz windows. *M* microammeter.
b) Photograph of the equipment. *L* box containing photoelectric cell.

[3] See Philips tech. Rev. **12**, 33-51, 1950.

with sulphide phosphors, that this may result in saturation of the fluorescence (see note[2])), but current density and focus are so adjusted that saturation cannot occur, or is so small that a correction can easily be made. The plate *P* and the wall of the tube *C* are connected together and are earthed across a microammeter *M*. Electrons leaving the layer of phosphor ultimately all arrive either on the plate *P* or on the cylinder *C*. At the commencement of the measuring operation electrons will also strike section *B* of the tube wall; this part is made of glass, but it has on the inside a layer of metal which is insulated from *A* and *C*. The layer is not earthed and therefore quickly acquires a sufficiently high negative potential to prevent secondary electrons from reaching this part of the tube. The current, as read from *M*, is then the primary electron current flowing to the plate *P*. The metal plate prevents the phosphor itself from acquiring a negative potential.

For observations on both sides of the screen, i.e. with the phosphors applied to glass plates, potentials of up to 10 kV were employed. No trouble was experienced as a result of charges on the screen.

The radiant energy of the fluorescence in the range of wavelengths 2000 Å — 7500 Å was measured with the aid of photo-electric cells which had been calibrated by comparison with a previously calibrated thermopile, using certain phosphors. Two vacuum photo-electric cells were used, a caesium antimony cell (having nearly constant sensitivity between 2500 and 5000 Å) and a rubidium cell (practically constant sensitivity between 5000 and 7000 Å). The first of these was employed for measurements on phosphors emitting blue or ultra-violet radiations, and the other for green, yellow or red fluorescence. In the latter instance, a separate test was necessary to ensure that no infra-red was present in the radiation, e.g. by repeating the measurement, this time with a filter passing only radiations of > 7500 Å. In some instances use was also made of a selenium barrier-layer cell. *Fig. 2* shows the relative spectral sensitivities of the photocells employed.

Most of the measurements were made with an acceleration voltage of 20 kV. The current density of the beam was about 1 μA/cm^2.

For reasons which will be mentioned later, it was found desirable to know the effect of the temperature of the phosphor on the efficiency, and for this purpose a tube was used of the kind depicted in *Fig. 3*. This tube contains a demountable cathode and, although provided with a focusing coil, has no deflection coils. The stationary beam is slightly converged, but is not sharply focused on the plate *P*. The temperature of the plate is raised by means of a heating element mounted underneath it and is measured with the aid of a chromel-alumel thermocouple attached to the plate. Secondary electrons either return to the plate *P* or are caught by the walls of the tube *C*, which are silver-plated, both being earthed through a microammeter. In this case, a tube *B*, internally silvered and insulated from the wall of *C*, has the same purpose as section *B* in fig. 1. A voltage of —100 V is applied to this electrode. The beam current employed was in general between 2 and 5 μA with an acceleration voltage of 8 kV.

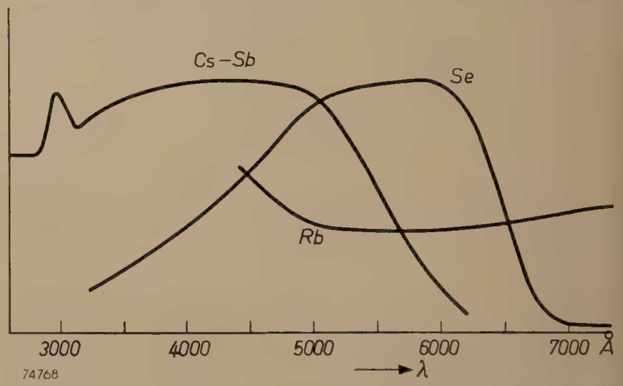

Fig. 2. Relative spectral sensitivities of the photo-electric cells used.

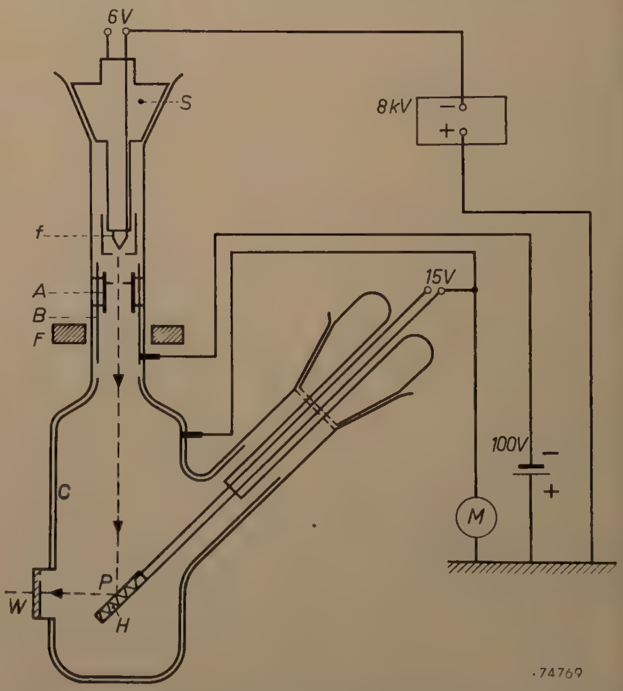

Fig. 3. Diagram of apparatus for the measurement of the efficiency as a function of the temperature. *S* stopper with interchangeable cathode *f*. *A* anode, *F* focusing coil, *B* and *C* internally silvered glass vessels, *W* quartz window, *P* target plate. H heating element, *M* microammeter. The temperature of the phosphor on the target plate is measured with a thermo-couple (not shown).

---

[4]) The lower limit of the wavelength range (2000 Å) was fixed by the transmissivity of the quartz windows.

Measurement of the efficiency

The absolute measurements of phosphor efficiencies are made with the aid of a calibrated thermopile, placed in front of window *a* (fig. 1), so that the light output in the direction normal to the phosphor layer is measured.

Denoting the area of the thermopile by S, the sensitivity by AS (watt/volt) and the voltage measured at the thermopile by v, the energy reaching the thermopile per second is thus ASv. This energy is emitted by the phosphor within a solid angle S/r^2 (r = distance thermopile to phosphor). The total energy radiated by the phosphor per second, having regard to Lambert's law and making a correction for the transmissivity τ of the window (a), is:

$$I = \pi r^2 Av/\tau. \qquad \ldots\ldots \qquad (5)$$

Let i_p represent the primary electron current and U the acceleration voltage; the energy I_p of the primary electron current flowing to P per second will then be $i_\mathrm{p}U$, and the efficiency:

$$\eta_\mathrm{m} = \frac{I}{I_\mathrm{p}} = \frac{\pi r^2 Av}{i_\mathrm{p} U \tau}. \qquad \ldots\ldots \qquad (6)$$

We have already seen above, how the intrinsic efficiency η_i can be derived from this measured efficiency η_m.

For a few phosphors the absolute efficiencies were determined in this way. The efficiencies of other phosphors were measured relative to these with the aid of the calibrated photocells described in the previous section.

Table I. Efficiencies of the fluorescence of a number of phosphors under electronic bombardment at 20 kV.

Phosphor	η_m %	R_∞ %	η_i %	$\frac{\mathrm{lm}}{\mathrm{W_r}}$	$\frac{\mathrm{lm}}{\mathrm{W_e}}$	Colour
$ZnS—10^{-4}Ag—Cl$	21			37	7	blue
$ZnS—5 \times 10^{-4}Ag —5 \times 10^{-4}Al$	23	83	25	35	8	blue
$(0.50\ Zn, 0.50\ Cd)S— 5 \times 10^{-5}Ag—Cl$	19.5			500	98	yellow
$ZnS—10^{-5}Cu—10^{-4}Al$	23	83	25	400	92	green
$ZnS—0.015Mn$	4	87	4.5	460	18.5	yellow
$ZnO—Zn$	7	85	7.5	340	24	green
$CaWO_4$	3	80	3.5	70	2	blue
$MgWO_4$	2	97	2	250	5	bluish
$CaO \cdot MgO \cdot SiO_2—0.03Ti$	7	91	7.5	70	5	blue
$Zn_2SiO_4—0.004Mn$	8.5	99	8.5	475	40	green
$2(88ZnO,12BeO)SiO_2— 0.02Mn$	7	97	7	450	31	yellow
$Cd_2B_2O_5—0.002Mn$	5.5	96	5.5	240	13	orange
$Cd_5Cl(PO_4)_3—0{,}05Mn$	7	95	7	400	28	orange
$Zn_3(PO_4)_2—0.3Mn$	5	100	5	170	8.5	red
$2CaO.Al_2O_3.SiO_2—0.04Ce$	4	90	4			blue

The results of a number of measurements are shown in *Table I*, in which the values in the first column are those of the measured efficiency η_m under the conditions mentioned. The second column shows the reflectivity R_∞ for light of the same spectral composition as the fluorescent light, and the third column the intrinsic efficiency η_i derived from the first and the second column. The fourth column contains the equivalent luminosity[5] (lm/W$_\mathrm{r}$) of the fluorescence, calculated from the spectral distribution, and the fifth column gives the product of the values in columns 1 and 4, i.e., the emitted luminous flux in lumens — per watt of the primary electrons (lm/W$_\mathrm{e}$). The sixth column gives an indication of the colour of the fluorescent light.

The sulphide phosphors ZnS-Ag-Cl and (ZnCd)S-Ag-Cl are generally employed for direct-vision television tubes; (ZnCd)S-Ag-Cl, (with less Cd than indicated in Table 1, giving greener fluorescence) is also used for the screen of the electron-microscope. Phosphors $CaO.MgO.SiO_2$-Ti and $2(ZnO.BeO)SiO_2$-Mn are used for the screens of projection television tubes. $CaWO_4$ is encountered in X-ray techniques.

Phosphors ZnO-Zn and $2CaO.Al_2O_3.SiO_2$-Ce are remarkable for their short persistence (10^{-6} and 10^{-7} sec respectively); these are used for the televising of films by the scanning method ("flying spot scanner") Zn_2SiO_4-Mn (willemite) is employed in oscilloscope tubes, and this (green luminescing) phosphor in conjunction with $Zn_3(PO_4)_2$-Mn (red) and $CaO.MgO.SiO_2$-Ti (blue) is of importance in certain colour-television systems.

The table also includes a number of other phosphors whose importance will become evident in the next section.

Effect of temperature on efficiency

It has already been seen that the bombardment of the screen by primary electrons results in only a part (η_i) of the energy being converted into radiation. The remainder is ultimately liberated at the screen in the form of heat. In the kind of tube used for large-screen projection television, in which the primary image is very small, the screen gets very hot and air-cooling is essential to prevent the temperature from becoming dangerously high. It is therefore useful to know how the efficiency of the fluorescence varies as a function of temperature.

---

[5] This has a value of 660 lumen/watt at the region of maximum visual sensitivity (5500 Å).

The temperature dependence of the fluorescence has been investigated in a number of different phosphors by means of the apparatus depicted in fig. 3. For the blue-fluorescing phosphors the measurements were made with the Cs-Sb vacuum photo-cell; for the phosphors the selenium cell was employed [6]).

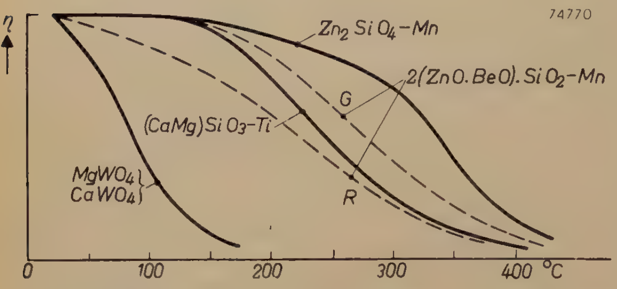

Fig. 4. Effect of temperature on the efficiency η of a number of phosphors. Curve *G* refers to the green, and *R* to the red band of the ZnBe phosphor.

As a rule a rapid decline in efficiency occurs above a certain temperature, but in some cases the drop is not so marked, or there may even be an initial increase.

A number of the results are shown graphically in *figs. 4* and *5*, in which the relative efficiency, i.e. 100 η/η_{max}, is plotted against the temperature in °C (η_{max} represents the maximum observed efficiency under prevailing conditions).

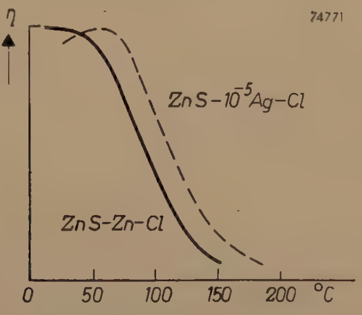

Fig. 5. Effect of temperature on the efficiency η of two sulphide phosphors.

Effect of the energy of the primary electrons on the efficiency

In addition to the above measurements, the variation in efficiency of certain phosphors with the energy of the primary electrons, or acceleration voltage, was determined. The results are reproduced in *fig. 6*, which shows the relative efficiency as a percentage (100 η/η_{max}) plotted as a function of the acceleration voltage in kV. (Here η_{max} represents the maximum measured efficiency under these conditions).

This maximum efficiency was in most cases attained with a voltage of 25 to 30 kV. For some phosphors the efficiency remains constant above that voltage, whereas with others it drops slightly on further increase of the voltage. There is no immediate explanation as to why this drop takes place; possibly it is due to an increasing influence of the absorption, since at higher voltages the electrons penetrate the layer of crystals to a greater depth — the fluorescent light accordingly has to travel further before being finally emitted. It is also possible that, when the primary electrons are accelerated, the chances of elastic collision are increased — at the expense of inelastic collisions — with a corresponding increase in the number of reflected primary electrons.

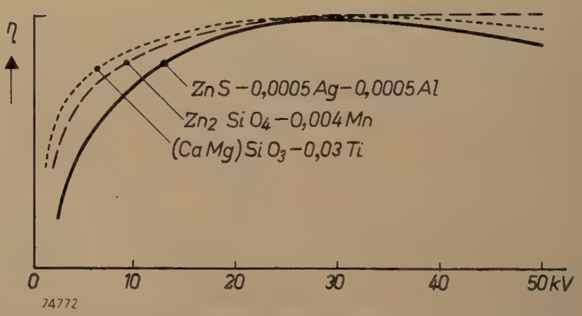

Fig. 6. Effect of the acceleration voltage on the efficiency η of various phosphors.

Comparison of cathodoluminescence with ultra-violet fluorescence

As will be seen from Table I, the efficiency of fluorescence due to electronic bombardment can be quite considerable, viz. up to 25%. This is particularly noteworthy in view of the many different ways in which energy is lost (elastic collisions, transitions without radiation etc.) mentioned in the introductory paragraphs.

Ultra-violet irradiation entails fewer causes of loss, and higher efficiency values are therefore often obtained. The quantum efficiency (chance of emission of a quantum of visible light per ultra-violet quantum absorbed) will quite frequently have values in the neighbourhood of 100%. However, since ultra-violet quanta embody more energy than the emitted light quanta, the energy efficiency, even in the most favourable cases, is naturally lower, being usually not more than 50%. *Table II* shows the efficiency of a number of phosphors when bombarded with electrons and also when irradiated with ultra-violet at wavelengths of 2537 Å and 3650 Å, from which it will be seen that, in terms of energy, the fluorescence of sulphides under electronic bombardment is well able to compete with that produced by U-V irradiation and in some instances is greater.

---

[6]) Actually, the spectral distribution does depend on the temperature (it usually increases in width when the temperature is increased), but, even allowing for the spectral variation of sensitivity of the selenium cell, no very great error is entailed in the measurement of the energy efficiency as a function of the temperature. At the same time, any such variation in the spectral distribution may have a marked effect on the colour of the fluorescent light.

Table II. Efficiency of the fluorescence of some phosphors under electronic bombardment and ultra-violet irradiation.

Phosphor	Energy efficiency		
	Electrons 20 kV	Radiation 2537 Å	Radiation 3650 Å
ZnS—5×10^{-4}Ag—5×10^{-4}Al	23	3	21
(ZnCd)S—Ag—Cl	19	10	35
ZnS—Cu—Cl	18	10	40
Zn_2SiO_4—Mn	8	45	—
$(ZnBe)_2SiO_4$—Mn	7	40	—
$MgWO_4$	2	45	—
$Cd_2B_2O_5$—Mn	5.5	35	—

Light yield from thin phosphor layers

In the foregoing we have shown how the efficiency η_i can be derived from the fluorescence of a very thick layer, with light emitted only from the rear. In practice, however, we are usually concerned with thin layers which are viewed from the front. The total luminous flux $\eta_i I_p = I_0$ produced (measured as energy) then gives rise to a luminous flux T emitted from the front of the layer, and another, R, emitted from the rear. In general:

$$R + T < I_0$$

because some of the radiant energy is lost by absorption in the layer. In *fig. 7* we give the theoretical curves for R, T and $R+T$ as a function of the layer thickness D (see Appendix), assuming that the electron energy I_p is wholly dissipated in the layer. Clearly, with very thin layers, half the light will be emitted from the front of the screen and half from the rear; hence when $D=0$, it may be said that, theoretically, $R=T=\frac{1}{2}I_0$, or, including a correction for reflection at the glass face, $R=\frac{1}{2}I_0\,(1+r_G)$, and $T=\frac{1}{2}I_0\,(1-r_G)$, where r_G denotes the reflection coefficient of the glass.

It will be seen that the luminous flux T, which is the important element, cannot exceed about 45% of the fluorescent radiation. In actual fact, in the case of very thin layers, the attainable values of T are even lower than those indicated in fig. 7, because thin layers cannot absorb the whole of the electron energy I_p. There are two reasons for this. If the layer thickness is less than the penetration depth of the electrons (about 1μ for 10 kV electrons), some of the primary electrons pass through the crystals without giving up their energy. Secondly, owing to the finite size of the crystals, holes occur in the layer if D (or strictly speaking, M, the weight per unit area of fluorescent substance), is very small. The penetration and, more particularly, the incomplete coating due to low values of M result in R and T both approaching zero. Since T, as we have already seen, also approaches zero with very thick layers (scatter and absorption), there must be an optimum layer thickness at which the luminous flux obtained at the front of the screen reaches a maximum. This is clearly demonstrated in *fig. 8*, in which measurements of R and T as

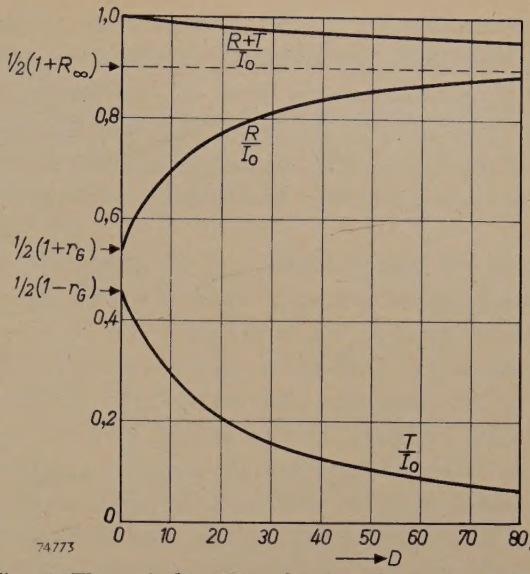

Fig. 7. Theoretical curves showing the ratio of luminous energy to intrinsic energy I_0 as a function of the thickness D. The upper curve refers to the total light output ($R+T$). The other curves are for the light emitted to the rear (R) and to that emitted to the front (T). The curves are computed from formulae (7) and (8) (see appendix; $a = 15$ cm^{-1}, $s = 600$ cm^{-1}, $R = 0.8$, $r_G = 0.08$).

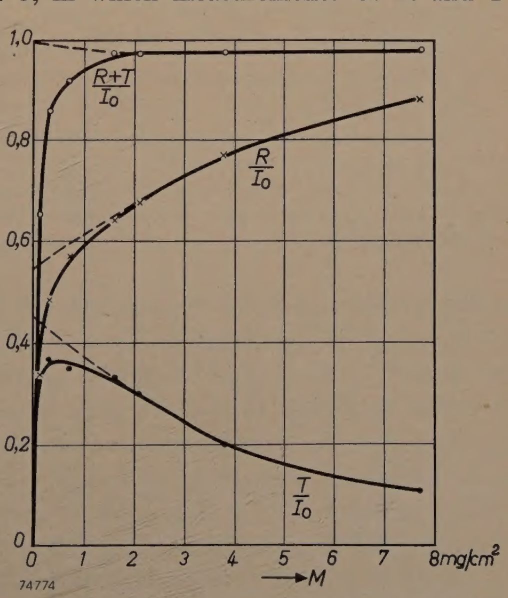

Fig. 8. Radiation from a willemite screen with 10 kV acceleration voltage, from the front (T) and rear (R), and the total ($R+T$), as a function of the coating M. The dotted lines are the theoretical curves shown in fig. 7.

applied to a willemite (Zn_2SiO_4-Mn) screen are shown graphically. With optimum layer thickness the energy T emitted at the front of the screen is usually 30 to 40% of the theoretical total fluorescent energy I_0. (At the rear we then have 60 to 65%; 5 to 15% is lost through the incomplete coating.)

Very much better results are obtained with a fluorescent screen having a metal backing, i.e. a thin film of metal on top of the phosphor. In some cases the metal backing is used to prevent the build up of charge on the screen (the metallic layer being earthed). It also largely protects the phosphor from bombardment by negative ions (ion burn), and it has yet another great advantage in that the light emitted towards the rear (R) is to a great extent reflected towards the front, thus adding to the effective luminous flux T.

The coating is applied in the following manner. A coating of some organic substance such as nitrocellulose is first produced on the layer of crystals by evaporation from a solution; this serves to fill up the interstices and irregularities, and thus to present a smooth surface. Aluminium is then evaporated on to this prepared surface, the organic filling layer being subsequently removed by heating, leaving the aluminium as a mirror-bright layer resting on the projecting corners of the crystals (*fig. 9*). The primary electrons now have to penetrate this layer, which is opaque to light, before they can reach the screen proper [7]). It is true that this involves a certain loss of energy (a few kV per micron of aluminium), but the gain in light due to reflection from the aluminium completely outweighs this; the reflection coefficient of the aluminium is very high (in the region of 80%; see Appendix).

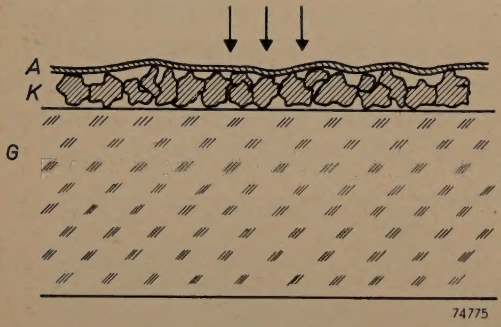

Fig. 9. Glass plate G with phosphor crystals K and aluminium backing A after removal of the nitro-cellulose layer. The arrows represent electrons.

A certain minimum thickness of aluminium is necessary before the reflection coefficient of the layer reaches this high value. On the other hand the layer may not be too thick for it would then absorb too much of the electron energy. This layer too, therefore has an optimum thickness. *Fig. 10* shows the quantity of light emitted (on a relative scale) from a thin willemite screen, plotted against the thickness of the aluminium layer; it will be noted that a maximum is reached with quite a thin layer of aluminium (some hundredths of a micron), this being followed by a gradual reduction as the thickness is increased. This drop is a result of the loss of energy of the primary electrons. Extrapolating to zero thickness, it is found that a loss of 10% occurs at 20 kV and 50% at 10 kV, both for 0.4 μ aluminium [8]). The optimum layer thickness is 0.02 — 0.08 μ for 10 kV, and about 0.1 μ for 20 kV.

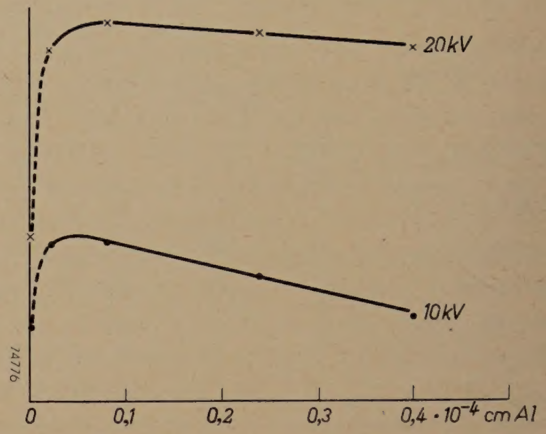

Fig. 10. Radiation (on relative scale) from the front of a willemite screen backed with aluminium, plotted against the thickness of the metal layer for 10 kV and 20 kV acceleration voltages.

A maximum in the light output of aluminized screens is also found with increasing thickness of the phosphor layer. This maximum would not occur if the reflection factor of the aluminium layer were 100% and if no light were lost through absorption in the phosphor layer: after being reflected once or several times by the aluminium all the light would finally be emitted from the front of the screen. The light output would thus increase with increasing thickness of the phosphor layer until the screen has become so thick that all the electron energy is being utilized, and would then remain constant. The reflection factor of the aluminium layer is, however, lower than 100%. This means that every time light falls on it some of it is absorbed. The thicker the phosphor layer i.e. the greater the value of R (see fig. 1), the more often the light is thrown back by the phosphor towards the aluminium layer and the higher the absorption losses become. The light output must approach zero at infinite thickness of the phosphor layer even if no losses occur through absorption in the phosphor layer itself. All the light is then lost in the reflection at the aluminium layer.

---

[7]) See J. de Gier, A projection television receiver, Philips tech. Rev. **10**, 97-104, 1948, in particular pp. 103-104.

[8]) With 50 kV and the same thickness, the loss in energy is only 1 to 2%. Cf. F. Kirchner. Ann. Physik ,**30**, 683-688, 1937.

If we compare the optimum values of T' (with aluminium) with T (without aluminium), we see that the gain amounts to a factor of 2 to 2.2.

In order to determine the light yield to be expected under the most advantageous practical circumstances it is necessary also to take into consideration the fact that, under manufacturing conditions, the efficiency of a phosphor is usually some 10% below its original value. Furthermore, the conditions under which tubes with sulphide screens are normally operated generally entail a certain amount of saturation, which results in a further loss of 10 to 15%.

The intrinsic luminous efficiency of a white-fluorescing sulphide mixture is roughly 60 lm/W, so that, in view of the above-mentioned losses, a mixture of this type can be expected to yield at most 15 lm/W at the front of the screen without metal backing, that is, a specific luminous intensity of about 5 cd/W, or 30 lm/W ($\approx$ 10 cd/W) with the backing.

The acceleration voltage necessary to produce these results must be at least 10 kV.

Appendix. Theoretical aspects of scatter and absorption

The scattering and absorption of light that take place in the screen can be formulated theoretically following Hamaker, Klasens, Coltman and others [9]), on the basis of a theory given by Schuster (1905).

This theory postulates that the characteristics of the screen are governed by two constants s and a, the first of which refers to the scattering and the second to the spectral absorption of the fluorescent light. It is assumed that the spectral composition of the fluorescent light is not modified by the absorption, so that s and a may be regarded as constant in a given instance. Furthermore, the phosphor layer is taken to be homogeneous, i.e. the grain size may be disregarded in comparison with the thickness of the screen.

According to Schuster, light scattering and absorption in a medium can be represented by the following differential equations:

$$\frac{\mathrm{d}J_1}{\mathrm{d}x} = -(a+s)\,J_1 + s\,J_2\,,$$

$$\frac{\mathrm{d}J_2}{\mathrm{d}x} = (a+s)\,J_2 - s\,J_1\,,$$

where J_1 and J_2 are the luminous flux values at a point x, in opposite directions perpendicular to the screen. At the rear of the screen ($x = 0$), J_2 is equal to R, and at the front ($x = D$), $J_1 = T$.

In the case of the scattering of fluorescent light R and T are evaluated by solving analogous differential equations, with the introduction of suitable boundary conditions. Using the abbreviated form $\sigma = [a(a+2s)]^{1/2}$ the relevant solutions for R and T are:

$$T = \tfrac{1}{2}\,I_0 \frac{1-r_G}{\dfrac{a+(1-r_G)s}{\sigma}\sinh\sigma D + \cosh\sigma D} \quad . \; . \quad (7)$$

$$R = \tfrac{1}{2}\,I_0 \frac{(1+r_G)\cosh\sigma D + \dfrac{(1-r_G)(a+2s)}{\sigma}\sinh\sigma D}{\dfrac{a+(1-r_G)s}{\sigma}\sinh\sigma D + \cosh\sigma D} \quad . \quad (8)$$

Further, it follows from the theory that:

$$\frac{s}{a} = \frac{2R_\infty}{(1-R_\infty)^2}\,, \quad . \; . \; . \; . \; . \; . \; . \; . \quad (9)$$

which, in conjunction with (7) and (8) enable us to write:

$$\frac{R}{T} = \frac{1+r_G}{1-r_G}\cosh\sigma D + \frac{1+R_\infty}{1-R_\infty}\sinh\sigma D\,. \quad . \quad (10)$$

Provided that σ D is sufficiently small (e.g. σ D $<$ 0.3), it may be said as an approximation that:

$$\frac{R}{T} = \frac{1+r_G}{1-r_G} + (a+2s)\,D\,. \quad . \; . \; . \; . \quad (11$$

The form of T and R are such that when $D \rightarrow 0$, $T = \frac{1}{2}I_0(1-r_G)$, and $R = \frac{1}{2}I_0\,(1+r_G)$; also $R + T = I_0$, as anticipated. If D be increased, T drops steadily and R rises. When $a = 0$, $R + T$ remains equal to I_0, since no energy is lost through absorption. When $a \neq 0$, while D increases, $R + T$ and also R alone, approach the value $\frac{1}{2}I_0\,(1+R_\infty)$, which agrees with the efficiency, given above, of $\eta_m = {}^1/_2\,(1+R_\infty)\eta_i$.

The functions (7) and (8) correspond closely to the experimental curves for $D \rightarrow \infty$, but this is no longer the case as $D \rightarrow 0$, because the electron energy is then not wholly absorbed by the phosphor layer.

The quantities s and a, which characterize the optical performance of the screen, are not usually known, so for a number of phosphors measurements have been taken of R, T, R_∞, r_G and D, from which a, s and σ have been computed with the aid of formulae (9) and (10), or (11); the results for the willemite screen (fig. 8) mentioned in the foregoing are now given in *Table III*.

Table III. Measurements on willemite (Zn_2SiO_4-Mn).

M mg/cm²	σ cm⁻¹	s cm⁻¹	a cm⁻¹
2	45	900	1
4	55	1100	1.5
6	65	1300	1.5
7.5	80	1650	2

It is thus seen that the values of σ and s are not constant, but depend on the layer thickness; the layers having $M = 2$ to 7 mg/cm² are in fact too thin for the theoretical formulae to be valid, while for the thicker layers measurements of T cannot be relied upon.

In principle it is also possible to compute the quantity of light using Hamaker's formulae in the case of screens with metal backing (reflection factor r_A); it is found that:

---

[9]) H. C. Hamaker, Philips Res. Rep. 2, 55-67, 1947.
H. A. Klasens, Philips Res. Rep. 2, 68-78, 1947.
J. W. Coltman, E. G. Ebbighausen and W. Altar, J. appl. Phys. 18, 530-544, 1947.
For further bibliography see note [1]).

$$T' = \tfrac{1}{2} I_0' \frac{(1-r_G)\,(1+r_A)}{\dfrac{(1+r_G r_A)a+(1-r_G)(1-r_A)s}{\sigma}\sinh\sigma D+(1-r_G r_A)\cosh\sigma D} \quad \ldots\ldots \quad (12)$$

where $I_0' = \eta_i I_p'$; $I_p' (< I_p)$ represents the energy of the primary electrons after they have passed through the aluminium layer. I_0' is therefore slightly less than I_0. In many cases the quantity r_G (roughly 8%) may be disregarded. Assuming that $\sigma D < 0.3$, our formula now becomes:

$$T' = \tfrac{1}{2} I_0' \frac{1+r_A}{1+[a+(1-r_A)s]\,D} \quad \ldots \quad (13)$$

Hence, if $r_A = 1$ and $a = 0$, we should find that $T' = I_0'$, in which case, as anticipated, all the light produced by the electrons would be emitted at the front, no matter how thick the screen were made.

When r_A differs from unity, the expected improvement can be computed with formula (12) or (13), the values of a, s and σ being taken from the actual measurements given above; conversely, r_A can be computed from measurements carried out on screens with and without aluminium backing.

With a given aluminium backing (0.3 μ thick) the relative efficiency of willemite was measured as a function of the layer thickness in mg/cm² of this phosphor; from the curve obtained for a voltage of 20 kV the magnitude of r_A was then determined with the aid of formula (13) in the form:

$$\frac{T_1'}{T_2'} = \frac{1+[a+(1-r_A)s]\,D_2}{1+[a+(1-r_A)s]\,D_1}, \quad \ldots \quad (14)$$

where D_1 and D_2 represent two values of the layer thickness, and T_1'/T_2' the ratio of the luminous emission values in respect of this thickness. For values of D_1 and D_2 corresponding to layers of 1.5 and 7.5 mg/cm² it was found that $T_1'/T_2' = 1.5$, so that $r_A = 0.83$. Direct measurement carried out on the aluminium layer after the tube had been opened, gave $r_A = 0.82$. In other cases the amount of agreement was not so close, but on the basis of a number of measurements taken, it may be said that r_A is roughly equal to 80%.

Summary. Introductory remarks on the mechanism of cathodoluminescence and the scattering and absorption of light in the screens of cathode-ray tubes are followed by a description of methods of measurement, the purpose of which is to determine the intrinsic conversion efficiency of electron energy into luminous energy. The results of measurements taken from a number of different phosphors with varying temperature and primary electron energy are presented. Further measurements give the luminous intensities at the front of conventional types of screen with and without aluminium backing. There are optimum values of the screen and backing thicknesses. Theoretical support is also lent to the arguments.

ABSTRACTS OF RECENT SCIENTIFIC PUBLICATIONS OF N.V. PHILIPS' GLOEILAMPENFABRIEKEN

Reprints of these papers not marked with an asterisk * can be obtained free of charge upon application to the address on the back cover.

2021: K. F. Niessen: Curie temperature of nickel-zinc ferrites as a function of the nickel-zinc ratio (Physica 17, 1033-1049, 1951).

In a series of mixed crystals of nickel ferrite (or any other ferromagnetic ferrite $Me^{2+}Fe_2O_4$) and zinc ferrite, the ratio of the Curie temperature to that of the zinc-free ferrite can be calculated by means of a generalisation of Néel's extension of the Weiss theory to ferrites. In this generalisation the interactions of all magnetic ions are taken into account. The dependence of the Curie temperature on composition leads to the prediction that zinc ferrite is antiferromagnetic.

2022*: H. G. Beljers, W. J. van de Lindt and J. J. Went: A new point of view on magnetic losses in anisotropic bars of ferrite at ultra high frequencies (J. appl. Phys. 22, 1506, 1951).

When ferrite rods are manufactured in a special way the magnetic losses at frequencies between 100 Mc/s and 10^4 Mc/s can be greatly reduced (in some cases down to 10 percent) by a relatively small, axially directed, magnetic field. Ferrite bars not specially manufactured show losses nearly independent of polarization. The effect may be explained by assuming that extrusion causes elongated air inclusions giving rise to an anisotropic structure, and a certain non-random orientation of the magnetic domains.

2023: A. M. Kruithof and W. de Groot: Photometry at very low brilliance levels (C.I.E. Proc., Stockholm 1951, Vol. 2,).

The paper describes preliminary experiments at luminances between 10 and 10^{-5} cd/m² with a photometer with circular field (central area 4°, annular area 8°) by four observers. A source, having a colour temperature of 2042 °K, is compared with sources of colour temperatures 2042 °K and 7700 °K resp. The heterochromous comparisons show a dependence on the fixation point (foveal and 4° parafoveal), which is apparent when the value of $\log (L_{2042}/L_{7700})$, corresponding to a match in apparent brightness, is plotted versus $\log L_{2042}$ (L = luminance).